# Geochemical and isotopic investigation into the source of U and Th enrichment in the Proterozoic, high heat producing granites of the Anmatjira Range

Thesis submitted in accordance with the requirements of the University of Adelaide for an Honours Degree in Geology

Jessica M Browne

November 2015

THE UNIVERSITY of ADELAIDE

# GEOCHEMICAL AND ISOTOPIC INVESTIGATION INTO THE SOURCE OF U AND TH ENRICHMENT IN THE PROTEROZOIC HIGH HEAT PRODUCING GRANITES OF THE ANMATJIRA RANGES

## HIGH HEAT PRODUCING GRANITES OF ANMATJIRA RANGES

## ABSTRACT

The Anmatjira Range of the North Australian Craton contains extraordinarily high heat producing Paleoproterozoic granites, with heat production being as high as 6.7$\mu Wm^{-3}$ as compared to the average upper crust of 1.69 $\mu Wm^{-3}$. Little previous research has been conducted as to the source of this enrichment of heat producing elements. This study investigates the degree of enrichment in these granites as well as their likely source.

Magmatic ages for the granitic suites were obtained by LA-ICP-MS, U-Pb geochronology along with inherited zircon ages of the suites which were compared with detrital ages of the Lander Rock Formation which is thought to have strong similarities with the source. The magmatic ages for the granites ranged from 1784 ± 6.6 to 1779 ± 9.9 Ma.

Whole rock geochemistry was used to compare heat production between the granites, as well as their dominant trends. All samples were peraluminous indicating a metasedimentary source.

A strong crustal influence on the granites is indicated by negative εNd values, however, as they are less negative than surrounding metasedimentary units there is a mantle influence on these granites.

The inherited zircons from the granites present a very similar (slightly younger) U-Pb age population to the oldest metasedimentary package in the area, the Lander Rock Formation.

These results support the initial hypothesis that an enriched crustal source with a mantle contribution formed these high heat producing granites. The inherited zircons strongly advocate that the already enriched source, with similarities to the Lander Rock Formation, is the most likely source rock.

## KEYWORDS

Geochemistry, Uranium, Thorium, Anmatjira Range, Heat Production

**TABLE OF CONTENTS**

## LIST OF FIGURES



## LIST OF TABLES

## 1. INTRODUCTION

In Northern Australia Proterozoic granites are uncharacteristically enriched in heat producing elements (HPE), with heat flow observed being 2 to 4 times higher than the average crustal estimates (McLennan and Taylor, 1996). HPE such as uranium (U) and thorium (Th) are considered to be highly incompatible in minerals that are characteristically sourced from the mantle, therefore, they typically accumulate in the continental crust (Bea, 2012). Bea (2012) suggested that the enrichment could be due to either: progressive extraction from the mantle, melting of an enriched source, or enrichment during partial melting.

The source rock is the main controlling factor when determining if a granite will be high heat producing (HHP) (Bea, 2012). Metasedimentary rocks will have a higher concentration of U, Th and K when compared to metabasic rocks. Therefore, metasedimentary material makes for a good crustal source for HHP granites. Bea (2012) summarised that most HHP granites are derived from a source which is already enriched in HPE.

Sandiford et al., (2002) proposed that the source of HHP granites of Australian Proterozoic was melting of a deep crustal source accompanied by additions to the lithosphere. This addition could serve two purposes: to act as a source material for the granites and/or to provide enough thermal input to melt the lower crust. McLaren & Powell (2014) researched the Proterozoic age HHP granites of the North Australian Craton (NAC). They proposed a model that, due to the long-term magmatic history of the Australian Proterozoic, these granites must have been the consequence of a hot-plate orogenic style that involved minimal crustal thickening as well as additional material

from a more juvenile magma. If this juvenile material was enriched in HPE it has the potential to greatly increase the heat production of the resulting granites when combined with an enriched crustal source.

HPE will preferentially stay in the crustal system thereby enriching the crust. When there is the addition of juvenile material any HPE will also become a part of the crustal system (McLaren & Powell, 2014). This addition and retention of HPE from juvenile mantle material helps account for a higher average heat production in younger granites observed across the Australian Proterozoic (McLaren & Powell, 2014).

Kromkun (2010) established that the source of the high heat producing Kalkadoon Supersuite was the result of underplating of an incompatible enriched mantle derived material which was accreted to the base of the lower crust.

Kromkun (2010) examined the mafic and felsic volcanic rocks of the Mt Painter Province in South Australia. The main aim of her study was to identify the source and petrogenesis of the high heat producing granites. By using a combination of whole-rock geochemistry, radiogenic isotopes and zircon geochronology she concluded that the crustal contaminated magma which generated the Mt Painter Province volcanics was formed by a combination of partial melting of the lower crust as well as a more mantle derived mafic magma. She also illustrated how fractional crystallisation of minerals such as plagioclase, K-feldspar and hornblende as well as a variety of accessory minerals is important in controlling the geochemistry of the magma.

Marshall (2013) researched how factors which influence HPE abundance will affect the overall elemental enrichment in HHP granites. She examined three HHP granite suites: The Big Lake Suite from South Australia, Cornwall in the U.K and Soultz-sous-Forets in France. In this study it was determined that the three main factors were: composition

of the source, degree of partial melting and the degree of fractional crystallisation. Marshall found that a low phosphorous content is conducive for developing HPE enrichments. It was also concluded that granites which formed in a within-plate, extensional setting, with minimal contribution from the mantle had the greatest enrichment of HPE.

This study focusses on the Anmatjira Range, part of the Aileron Province. Magmatism within the Aileron Province occurred over the period of 1820 – 1700 Ma (Scrimgeour, 2013). In the Anmatjira Range there is evidence of multiple generations of granitic magmas from a single lithospheric column.

The primary aim of this project is to investigate how mantle derived material and intracontinental recycling relate to result in the development of the oldest HPE enriched granites in the Aileron Province and identify the potential source rock.

This study will aim to provide a greater database of zircon geochronology for three granitoid suites of the Anmatjira Range. Inherited zircon U-Pb ages, in conjunction with detrital zircon data from previous studies, will be used to compare age populations with those of the basement or older metasedimentary rocks of the Aileron Province. Geochemical and isotopic data, will be used to determine the extent of influence that each of the crust and the mantle had on these granites. Results from this study have significance in supplementing our knowledge of how Proterozoic Australia became so extraordinarily enriched in HPE.

# 2. GEOLOGICAL SETTING

## 2.1 North Australian Craton

The North Australian Craton (NAC), located predominantly in the Northern Territory, consists of Paleoproterozoic aged, poorly delineated cratonic blocks (Cawood and Korsch, 2008). With limited outcrop, an Archean basement is inferred from geophysical data sets, from Shaw et al (1995) & Cawood and Korsch (2008).

## 2.2 Arunta Region

Situated in the south of the NAC is the Arunta Region, a late Paleoproterozoic, broadly E-W trending, metasedimentary and volcanic assemblage (Collin and Shaw, 1995, Cawood and Korsch, 2008, Anderson et al., 2013) (Figure 1). The Arunta Region is divided into three provinces: The Aileron, Warumpi and Irindina (Anderson et al., 2013). The Aileron Province, located in the north of the Arunta Region, is a Paleo-Mesoproterozoic orogenic domain, (Claoue-Long et al., 2008a) (Scrimgeour, 2003). The Aileron Province experienced a complex tectonic history, with six tectonothermal cycles spanning 1820 – 300 Ma (Anderson et al., 2013). The Stafford Tectonic Event 1820 Ma and the Strangways Orogeny 1770-1780 Ma both resulted in low-pressure greenschist to granulite facies metamorphism (Hand and Buick, 2001). These events have been associated with the emplacement of the granites in the Reynolds-Anmatjira Ranges (Hand and Buick, 2001). Depositional ages range between 1860 and 1700 Ma (Scrimgeour, 2003).

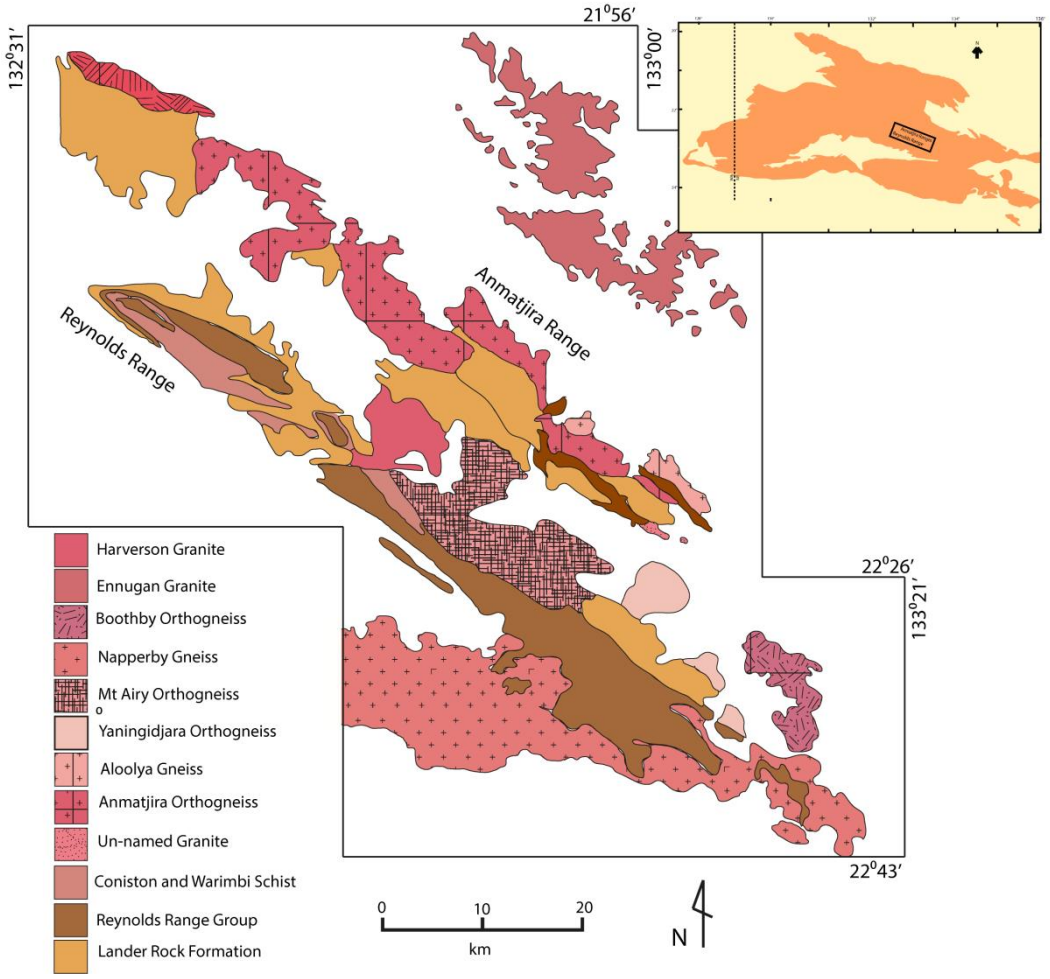


**Figure 1. Generalised geology of the Reynolds-Anmatjira Ranges, modified after Hand M & Buick IS, (2001). Insert of the Arunta Region in central Australia, with the location of the Anmatjira and Reynold Ranges in the central Aileron Province, (modified after Scrimgeour, 2013).**

### 2.3 Anmatjira Range

The Anmatjira Range is NW-SE trending and is situated in the middle of the Aileron Province, just north of the adjacent Reynolds Ranges (Anderson et al., 2013). It is composed of metasedimentary basement packages, charnockites and granitoids, all of which have experienced the before mentioned metamorphic events and consequent deformation. The oldest known package in the Ranges is the Lander Rock Formation which is a turbiditic, quartzose and relatively Mg-rich pelitic metasedimentary package (Cawood and Korsch, 2008, Claoue-Long et al., 2008a, Hand and Buick, 2001). U-Pb

ages from previous studies show detrital zircon age populations for the Lander Rock Formation to be between 1880-1840 Ma (Cawood and Korsch, 2008).

Within the Anmatjira Range there are a large number of foliated to gneissic megacrystic granites including: the Aloolya Gneiss, Anmatjira Orthogneiss, Possum Creek Charnokite, Harverson Granite, Mount Airy Orthogneiss, Yaningidara Orthogneiss and an Un-named Granite (Scrimgeour, 2013) (Figure 1). These granites intrude the Lander Rock Formation in multiple locations throughout the Anmatjira Range.

In the south of the Anmatjira Range lies the tourmaline and granite bearing Aloolya Gneiss. From U-Pb dating the Aloolya Gneiss has been restrained to 1807 ± 6 Ma (Scrimgeour IR, 2013). There is a cuspate intrusive contact between the Aloolya Gneiss and the Anmatjira Orthogneiss (1802-1794 Ma), which suggest that the Anmatjira Orthogneiss was still molten when the Aloolya Gneiss intruded (Rösel et al., 2014) (Scrimgeour, 2013).

## 3. ANALYTICAL METHODS

### 3.1 Field Work/ Sample Preparation

Samples in this study were collected in the Anmatjira Range from outcrops with minimal deformation and weathering. Samples AMJ-GP-11, AMJ-GP-26 and AMJ-GP-28 were sand samples collected from dry creek beds.

Three gamma ray spectrometers were used in the field, with a collection time ranging from 100 – 180 seconds. Data was collected for K (%), U and Th (ppm), using the assay mode on each device. Outcrops needed to be a minimum of half a cubic metre as this is the active detection area capability for these particular devices.

Cut blocks from 31 samples were sent to Lab Crystals/Continental Instruments in India where thin sections were produced, to be used for mineral petrography.

Zircons were separated via hand panning and magnetic separation techniques and then mounted in epoxy resin. All zircons were imaged using Back Scatter Electron and Cathode Luminescence detectors on a Philips XL-20 SEM.

Samples were crushed and milled and then sent to ALS Minerals for whole rock geochemical analyses. Data analysis was conducted using GCDkit software.

### 3.2 U-Pb Geochronology

The LA-ICP-MS procedures used in this project are similar to those of Payne et al. (2006). $^{206}$Pb, $^{207}$Pb, $^{208}$Pb, $^{232}$Th and $^{238}$U were analysed, while $^{235}$U was calculated from $^{238}$U, by using a $^{238}$U/$^{235}$U ratio of 137.88. $^{204}$Pb was also monitored to determine any influence common Pb may have on the results. The zircon standard GJ-1 was used as a primary standard to correct for mass bias and fractionation. All data correction was conducted via the Glitter software, developed by Macquarie University. For the purpose of this project a linear fit algorithm was used to account for mass spectrometer drift. Data quality was monitored using the Plesovice zircon standard (337.13 ±0.37 (Sláma et al., 2008). The beam size used was 30µm with a 5 Hz repetition and energies of 55%.

### 3.3 Radiogenic Isotopes

Sm-Nd isotope analyses were conducted at the University of Adelaide, using the method outlined in Payne et al. (2006). A $^{150}$Nd/$^{147}$Sm solution was used to spike the samples and dissolution was carried out in Teflon vessels over a 7 day period at 160 °C. REE were separated in Biorad Polyprep columns, and then further separated in impregnated Teflon-powder columns in order to isolate Sm and Nd. The Nd isotopes

were analysed on a Finnigan MAT 262 Thermal Ionisation Mass Spectrometer (TIMS) with an in-house Nd standard (Johnson Matthey, 143Nd/144Nd=0.511604 ±0.000008). Sm was analysed on a MAT 261 TIMS.

# 4. OBSERVATIONS AND RESULTS

## 4.1 Sample and Petrography Descriptions

### 4.1.1 ANMATJIRA ORTHOGNEISS

Twenty one samples were collected from the Anmatjira Orthogneiss. Three of these samples (AMJ-GP-11, AMJ-GP-26 and AMJ-GP-28), were sand samples collected from dry creek beds. Two variations of the Anmatjira Orthogneiss outcrop were observed in the field: a megacrystic and a fine grain variation (Figure 2c & d). Both variations were dominated by plagioclase, K-feldspar, biotite and quartz. While both variations contain garnet there was a greater abundance observed in the megacrystic variation. However in sample AMJ-GP-23 no garnet was visible in outcrop.

In thin section all samples contained biotite, quartz and muscovite, while most samples had plagioclase, k-feldspar and muscovite. Small grains of zircon could be observed in certain samples such as AMJ-GP-08 and 09. The majority of samples contained microcline and perthite showing varying degrees of weathering and deformation. Cordierite and garnet was also observed in small quantities in some samples (Figure 3b).

Texturally the megacrystic outcrops also contained rapakivi of K-feldspar surrounded by biotite. Most outcrops in the Anmatjira Range had experienced metamorphism and displayed an E-S-E to W-N-W trending foliation defined by biotite.

The mafic association of the Anmatjira Orthogneiss in thin section is dominated by hornblende, and contains clinopyroxene ± magnetite/hematite (Figure 3a).

Samples AMJ-GP-08, 09 and 10 were collected from Aloolya Springs. In this field location granites with mafic enclaves as well as cross cutting pegmatites were observed. The pegmatite represents the last stages of fractionation in the system, and demonstrated a gradational boundary with the Anmatjira Orthogneiss (Figure 2d). The pegmatites mineralogy was dominated by quartz, biotite and plagioclase. Multiple mafic enclaves were also observed at this location intruding the granite (Figure 2d).

The field location of sample AMJ-GP-17 also had pegmatite veins consisting of orthopyroxene and was transitional into the Possum Creek Charnockite, as well as rapakivi reaching up to 10 cm in length.

### 4.1.2 ALOOLYA GNEISS

Ten samples were collected across the Anmatjira Range from the Aloolya Gneiss, four of which were mafic associations. A garnet-biotite bearing augen gneiss, outcrops were dominated by glassy garnet, biotite, K-feldspar and quartz. Similar to the Anmatjira Orthogneiss there were two variations observed in the field: a coarse grain and a finer grain variety. The coarser grain outcrops were rich in garnet, biotite, plagioclase and contained many rounded k-feldspar (Figure 2e). The finer grained outcrops contain a higher content of quartz and also contained tourmaline, however not all fine grain outcrops contained tourmaline.

In thin section symplectic intergrowths were observed (Figure 3d). Groundmass was dominated by quartz, while muscovite appears to grow in veins around other minerals. Cordierite and zircon were observed in multiple samples.

Observed in some of the outcrops was a S-E to N-W foliation which was defined by the biotite. The mafic associations and enclaves contained pink feldspar ranging 7 to 12 mm in length.

A gradational transition was observed in the field from the Possum Creek Charnockite to the Aloolya Gneiss. Moving from the charnockite to the gneiss orthopyroxene slowly transitioned out and was replaced by biotite, garnet and tourmaline.

### 4.1.3 UN-NAMED GRANITE

Located in the S-E of the Anmatjira Range is a garnet-bearing granite which has no assigned formation name. Three samples were collected. Outcrops were extremely weathered and were dominated by quartz, biotite, garnet and K-feldspar (Figure 2g). Quartz veins were observed in the outcrops (Figure 2g & h). At the field location where sample AMJ-GP-34 was collected mylonites were observed.

In thin section, samples were dominated by garnet, plagioclase and quartz. There was also biotite, zircon magnetite, and in sample AMJ-GP-34 sericite. Symplectic intergrowths were observed in all three samples.

This granite is extremely rich in garnet, especially magnetic garnet which was separated out using a Franz.

### 4.1.4 POSSUM CREEK CHARNOCKITE

Three samples were collected in the field of the Possum Creek Charnockite. Outcrops were dominated by biotite, k-feldspar, plagioclase and extremely weathered orthopyroxene, with rapakivi (Figure 2a). Outcrops presented a SE-NW trending metamorphic foliation which was defined by biotite. Sample AMJ-GP-10 contained many large K-feldspar grains, while sample AMJ-GP-20 was an ultra-fine variation.

In thin section all samples combined biotite, quartz, muscovite and plagioclase (Figure 3g & h). Sample AMJ-GP-10 was the only sample which contained phenocryst K-feldspar with its groundmass consisting of quartz, plagioclase and K-feldspar. Sample AMJ-GP-18 and 20 also had orthopyroxene, microcline, perthite and sericite. Samples AMJ-GP-18 and AMJ-GP-20 consisted mainly of groundmass of muscovite, biotite, quartz and plagioclase, with some larger grains of plagioclase and quartz.

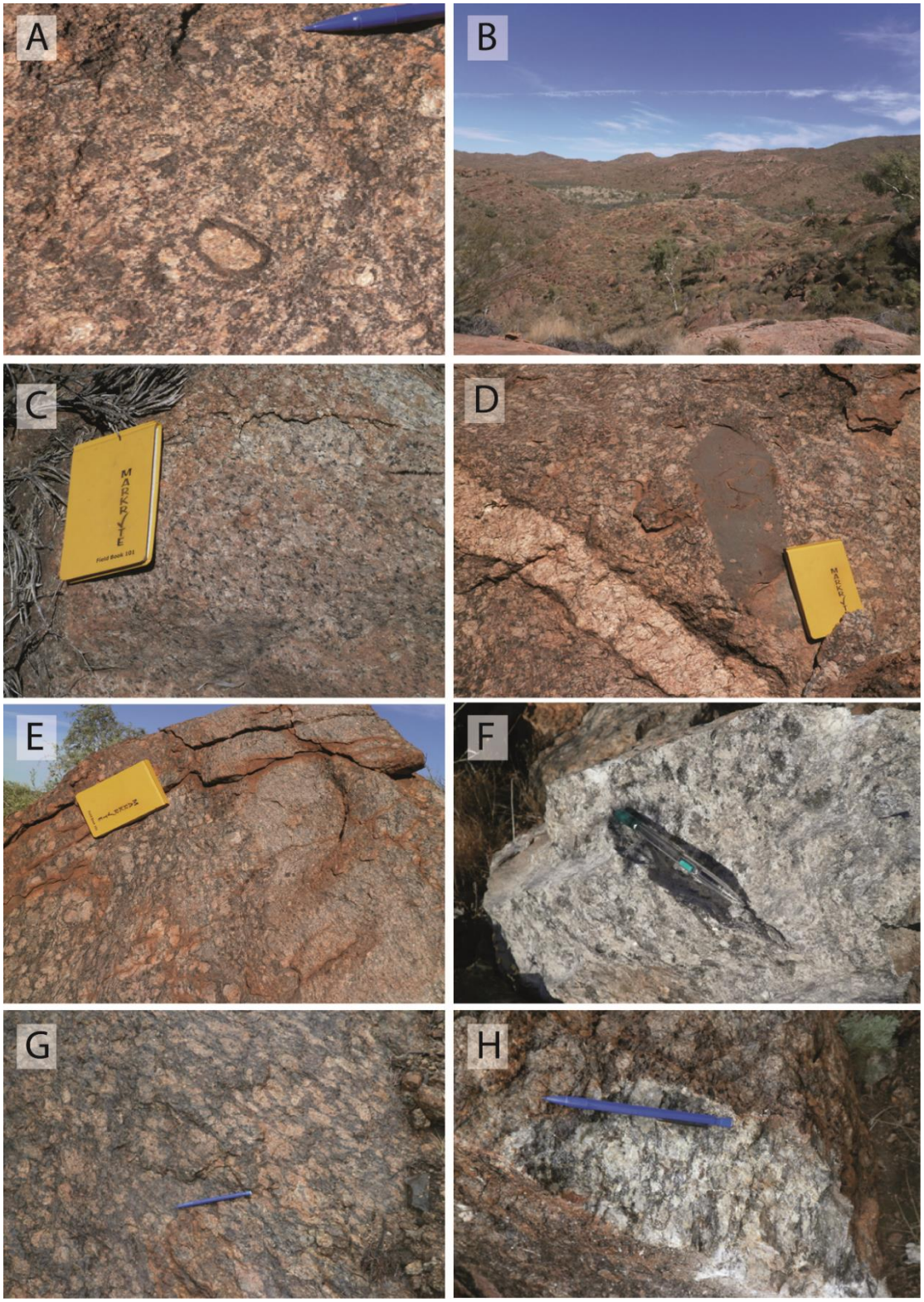


**Figure 2. Field photographs from the Anmatjira Range a) Possum Creek Charnockite with rapakivi, b) expanse of the Anmatjira Orthogneiss, c) fine grained Anmatjira Orthogneiss, d) megacrystic Anmatjira Orthogneiss, with mafic enclave and pegmatite, e) Aloolya Gneiss showing both fine and, f) course grain Aloolya Gneiss, g) weather outcrop of the Un-named Granite, h) fresh outcrop of the Un-named Granite**

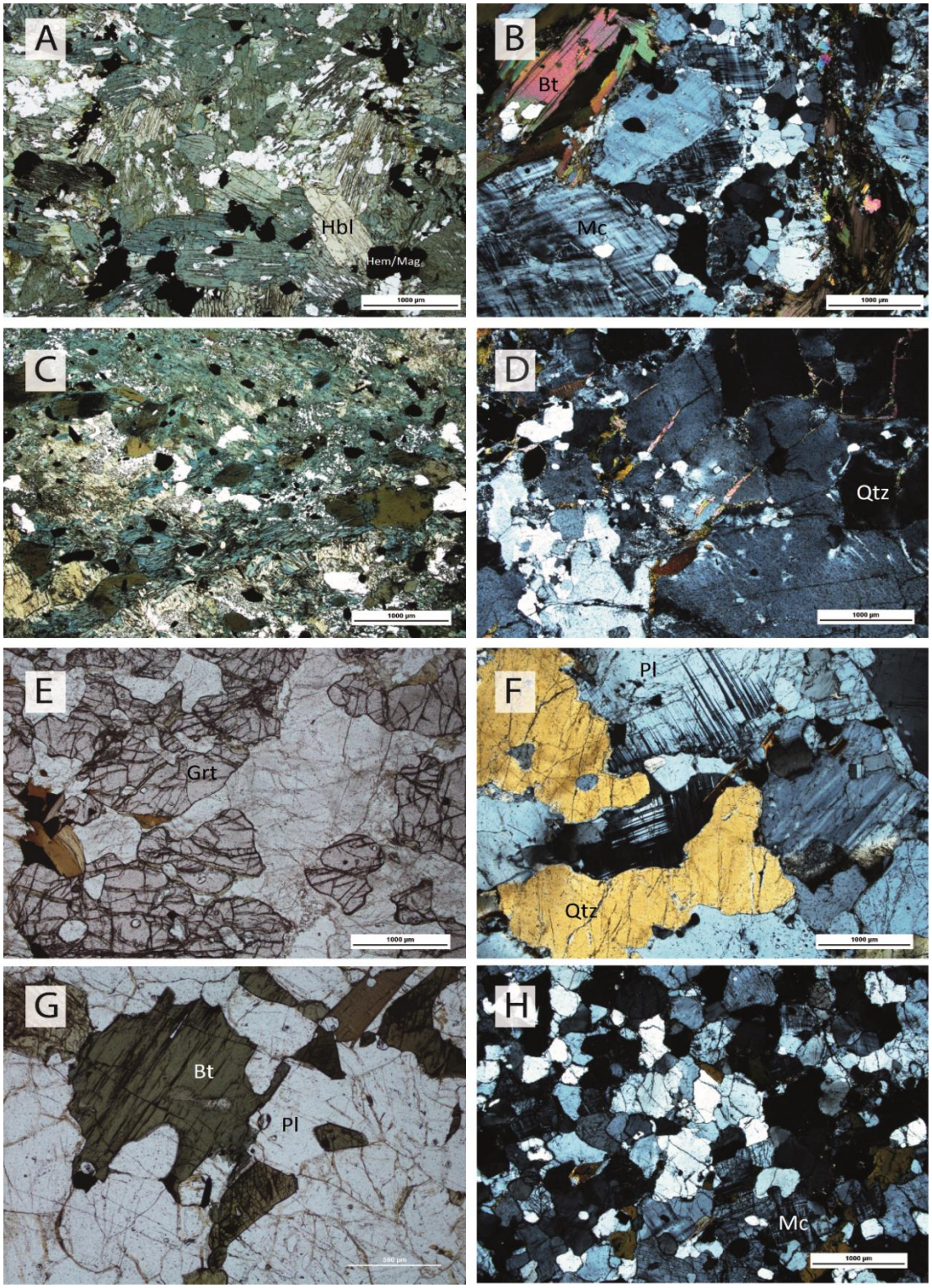


**Figure 3. Representative photo micrographs of granites and Charnockite of the Anmatjira Range a) PPL of a mafic association of Anmatjira Orthogneiss, b) typical mineralogy and textures of Anmatjira Orthogneiss in XPL, c) mafic association of the Aloolya Gneiss in PPL, d) representative textures and mineralogy of Aloolya Gneiss in XPL, e) PPL image of Un-named granite, showing abundance of garnet in the sample, f) typical XPL of minerals and textures of the Un-named Granite, g) PPL image of Possum Creek Charnockite, h) XPL image of Possum Creek Charnockite.**

When plotted on a plutonic rock classification diagram, samples from the Anmatjira Orthogneiss, Aloolya Gneiss and the Possum Creek Charnockite fall in the granite field. Samples from the Un-named Granite fall in both the granite and quartz monzonite fields. Samples which are mafic associations fall in either the gabbro or gabbroic diorite fields (Figure 4).

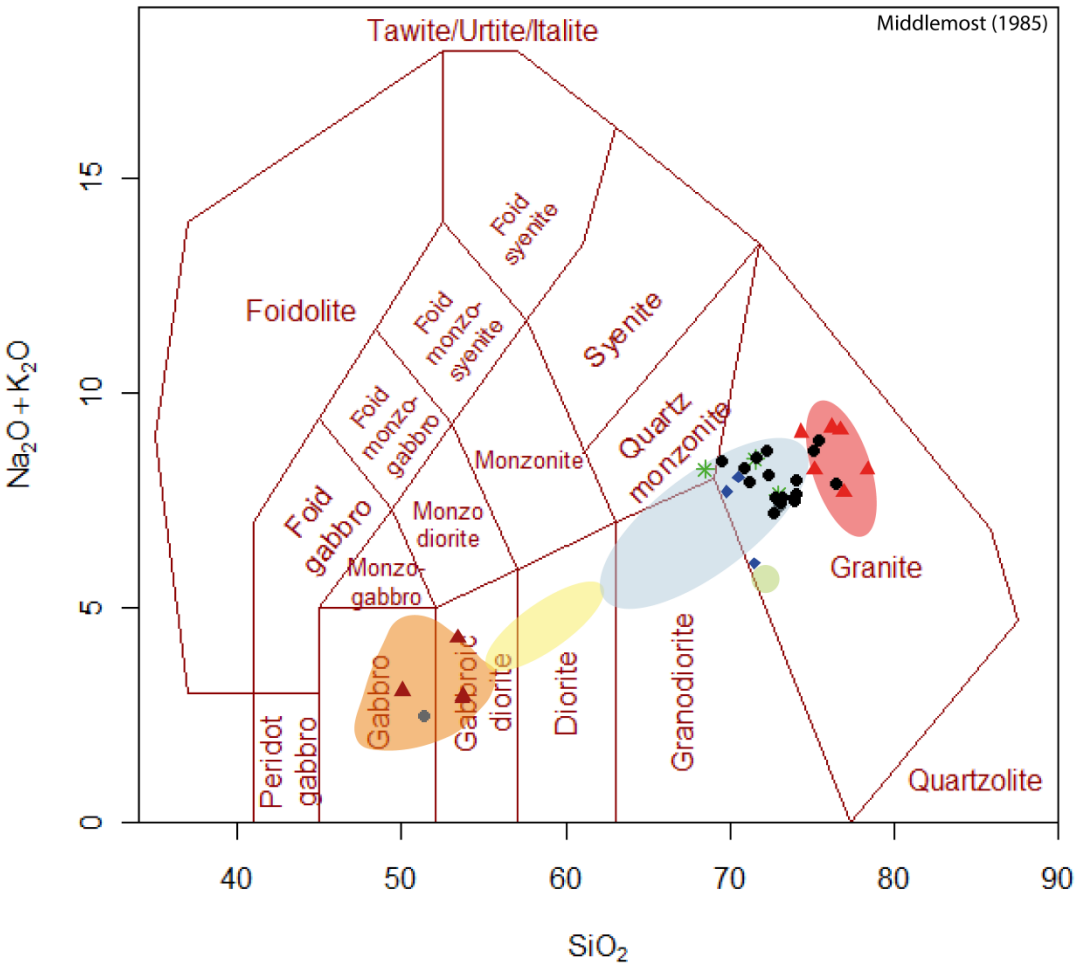


**Figure 4. A classification plot, after Middlemost 1985. Anmatjira Orthogneiss (black circles), Aloolya Gneiss (red triangles), Un-named Granite (green stars), Possum Creek Charnockite (blue diamonds), mafic association of the Anmatjira Orthogneiss (grey circles) and the Aloolya Gneiss (maroon triangles). The blue fields represents data from Possum Creek Charnockite, the green field Mylonite from the Possum Creek Charnockite, yellow fields representing data from Tyson Creek Granulite (mafic), red field representing data from Tyson Creek Granulite (felsic) and the orange field representing the Tyson Creek Granulite mafic/felsic association J Hopkinson (2015 per. comm., 1 July).**

### 4.2 U-Pb Geochronology

U-Pb geochronological analyses were undertaken on five samples from the Anmatjira Range. Zircons which exhibited discordancy (>10%) or elevated concentrations of $^{204}Pb$ (common Pb) (significantly higher than the standards) were discarded and not included in age calculations. U-Pb Concordia ages are presented in Figure 5 as well as weighted average $^{207}Pb/^{206}Pb$. A full table of all results can be found in Appendix C. Based on Cathodoluminescence (CL) images, ages presented are either magmatic or inherited, as shown by cores surrounded by oscillatory zoning which are present in some of the zircons (Figure 5).

**Table 1. Summary of magmatic ages from zircon geochronology for samples from the Anmatjira Range**

| Geological Unit | Sample ID | Rock Type | Easting | Northing | Cryst. Age (Ma) |
|---|---|---|---|---|---|
| Anmatjira Orthogneiss | AMJ-GP-01a | Granite | 291157 | 7542522 | 1784.9 ± 6.6 |
| Aloolya Gneiss | AMJ-GP-19 | Granite | 300015 | 7534215 | 1779 ± 9.8 |
| Un-named Granite | AMJ-GP-36 | Granite | 306867 | 7523160 | 1780 ± 7.5 |

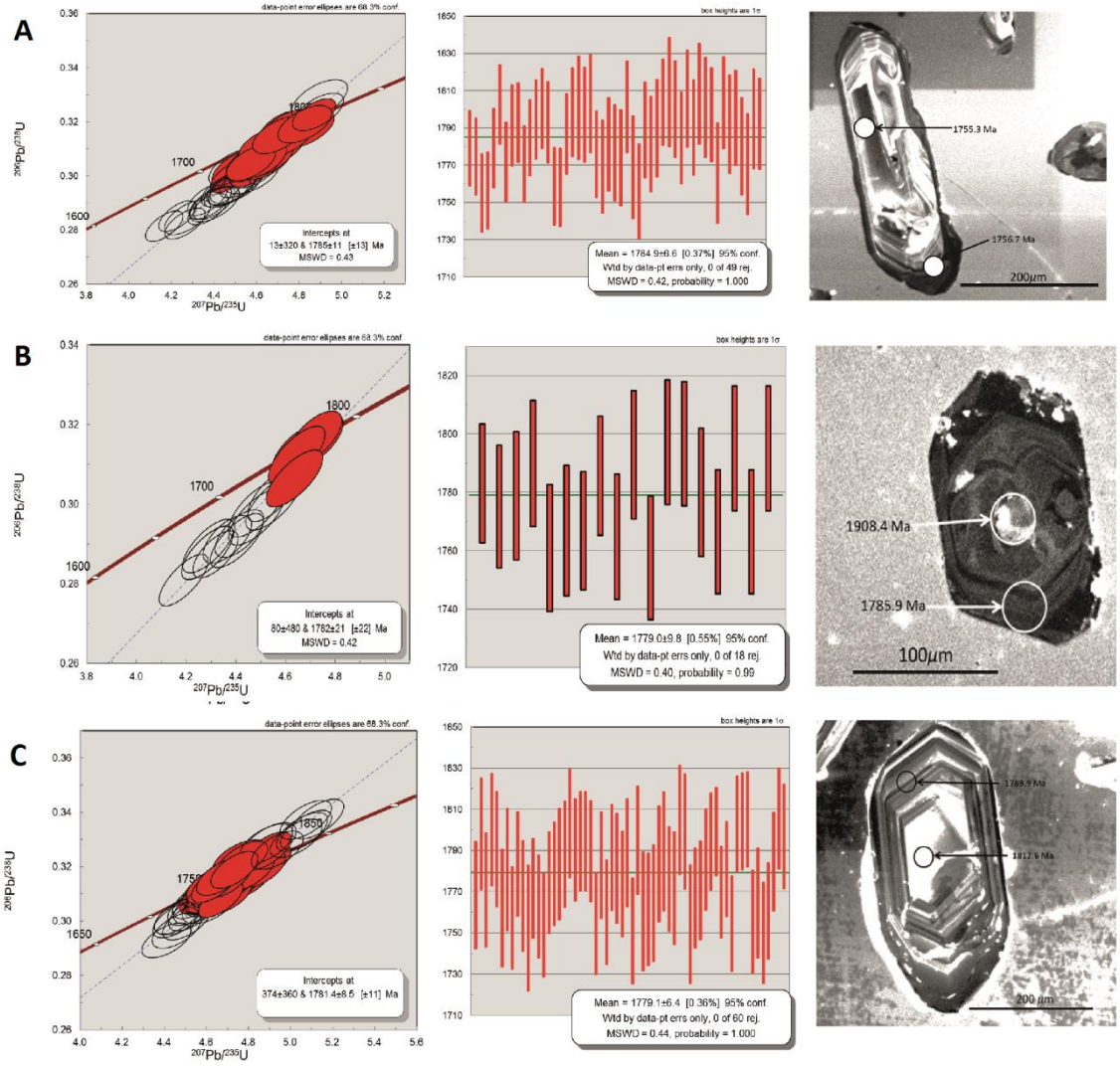


**Figure 5. Concordia plots, 207Pb/206Pb weighted average plots and represented CL images for zircons from each sample. a) sample AMJ-GP-01a Anmatjira Orthogneiss, b) AMJ-GP-19 Aloolya Gneiss, c) AMJ-GP-36 Un-named Granite**

### 4.2.1 ANMATJIRA ORTHOGNEISS

#### Sample AMJ-GP-01a

Zircons extracted from the Anmatjira Orthogneiss range in length from 50$\mu$m to 400$\mu$m. The zircons morphology was dominated by elongated, euhedral to subhedral grains. CL imaging revealed a variety of textures and relationships including: core-rim relationships, oscillatory zoning, metamorphic overprinting and metamictization. One hundred and eight five analyses were collected to deduce a crystallisation age. Of these

forty-nine analyses were used. The analyses spread of $^{207}Pb/^{206}Pb$ ages ranged 1755.3 to 1809.4 Ma, with a weight mean $^{207}Pb/^{206}Pb$ age of 1779.0 ± 9.8 Ma (Figure 5a). Ages of suspected inherited cores range from 1828.7 to 2257.4 Ma (Figure 5a).

### Sample AMJ-GP-11

Fifty-three analyses were conducted, of which fourteen were used to determine the age of crystallisation. This produced a range of $^{207}Pb/^{206}Pb$ ages from 1751 to 1803.3 Ma. A weighted mean of this data produced a $^{207}Pb/^{206}Pb$ age of 1784 ± 12 Ma, with a MSWD of 0.56. Overall for this sample there was a wide range of ages ranging from 1605.75 to 1790.7 Ma.

### Sample AMJ-GP-28

One hundred and forty three analyses were collected, eighteen of which were used. From these analyses there were a spread of $^{207}Pb/^{206}Pb$ ages ranging from 1782.3 to 1815.6 Ma, and the weighted mean was 1798 ± 11 Ma. There was a large spread of ages for this sample ranging from 1531 to 2189.5 Ma.

## 4.2.2 ALOOLYA GNEISS

### Sample AMJ-GP-19

Zircons ranged in size from 50$\mu$m to 400 $\mu$m. The morphology ranged from euhedral crystal shape, while others presented a more rounded appearance. CL imaging revealed a core-rim relationship in many zircons (Figure 5b). Other relationships included a metamorphic overprinting of the oscillatory zoning as well as zircons which appear to have formed entirely during metamorphic events. Some grains had also undergone metamictization.

One hundred and seven analyses were conducted to deduce a crystallisation age for the Aloolya Gneiss. Of these forty four analyses were used, creating a spread of $^{207}Pb/^{206}Pb$ ages from 1757.8 to 1796.8 Ma. A weighted mean $^{207}Pb/^{206}Pb$ age of 1779 ± 9.8 Ma (95% confidence) and a MSWD of 0.23 was obtained (Figure 5b). These targeted areas of zircon grains either presented oscillatory zoning or were very bright, suggesting a high uranium content. Inherited cores of the zircons yielded $^{207}Pb/^{206}Pb$ age peaks ranging from 1828.7 to 2225.4 Ma, and an overall spread of ages which include both inherited and metamorphic ages ranging 1531 – 2189.5 Ma.

#### 4.2.3 UN-NAMED GRANITE

##### Sample AMJ-GP-36

Zircons ranged in size from 60 $\mu$m to 420 $\mu$m, with morphology ranging from euhedral to subhedral.

Many of the zircons also presented an inherited core surrounded by oscillatory zoning. One hundred and twenty seven analyses were conducted of which sixty were used to determine a crystallisation age. $^{207}Pb/^{206}Pb$ ages ranged from 1751.2 to 1805.8 Ma. A weighted mean $^{207}Pb/^{206}Pb$ age of 1779 ± 6.4 Ma (95% confidence) and a MSWD of 0.44 was obtained (Figure 5c). Zircons with inherited cores yielded $^{207}Pb/^{206}Pb$ age peaks ranging from 1832.75 to 3119 Ma.

### 4.3 Whole Rock Geochemistry

#### 4.3.1 MAJOR ELEMENTS

A full report of whole rock geochemistry is found in Appendix B. The Anmatjira Orthogneiss ranges from 70.1 to 78.8 wt% $SiO_2$, the Aloolya Orthogneiss ranges from

76.6 to 80.4 wt% $SiO_2$, the Un-named Granite ranges from 71.9 to 72.9 wt% $SiO_2$, and the Possum Creek Charnockite ranges from 69.3 to 73.3 wt% $SiO_2$ (Figure 7) . $Al_2O_3$, $Fe_2O_3$, CaO, MgO and $TiO_2$ all decrease in abundance as $SiO_2$ increases, while $P_2O_5$, $Na_2O$ and $K_2O$ appear to have considerably more scatter when compared to $SiO_2$ (Figure 7).

Figure 8 illustrates the relationship between elemental enrichments with increasing fractionation. Nb, Zr and Th all have negative correlations, where with increasing fractionation the elements decrease in abundance. Rb and U show a slight increase in abundance with increasing fractionation. Y shows a lot of scatter and no distinct trend in abundance with increasing fractionation.

The majority of samples are enriched in K and therefore plot as peralumious on the Alumina Saturation Index as they have an A/CNK value which is greater than one (Figure 9).

### 4.3.2 TRACE ELEMENTS AND RARE EARTH ELEMENTS

Figure 10 shows depletions in Sr, Ba and En compared to the other REE. REE patterns from all samples have a negative Eu anomaly ranging from slight to large anomalies (Figure 11). The majority of samples are enriched in LREE compared to a flat HREE trend (Figure 11). Sample AMJ-GP-04 from the Aloolya Orthogneiss has very low concentrations of HREE.

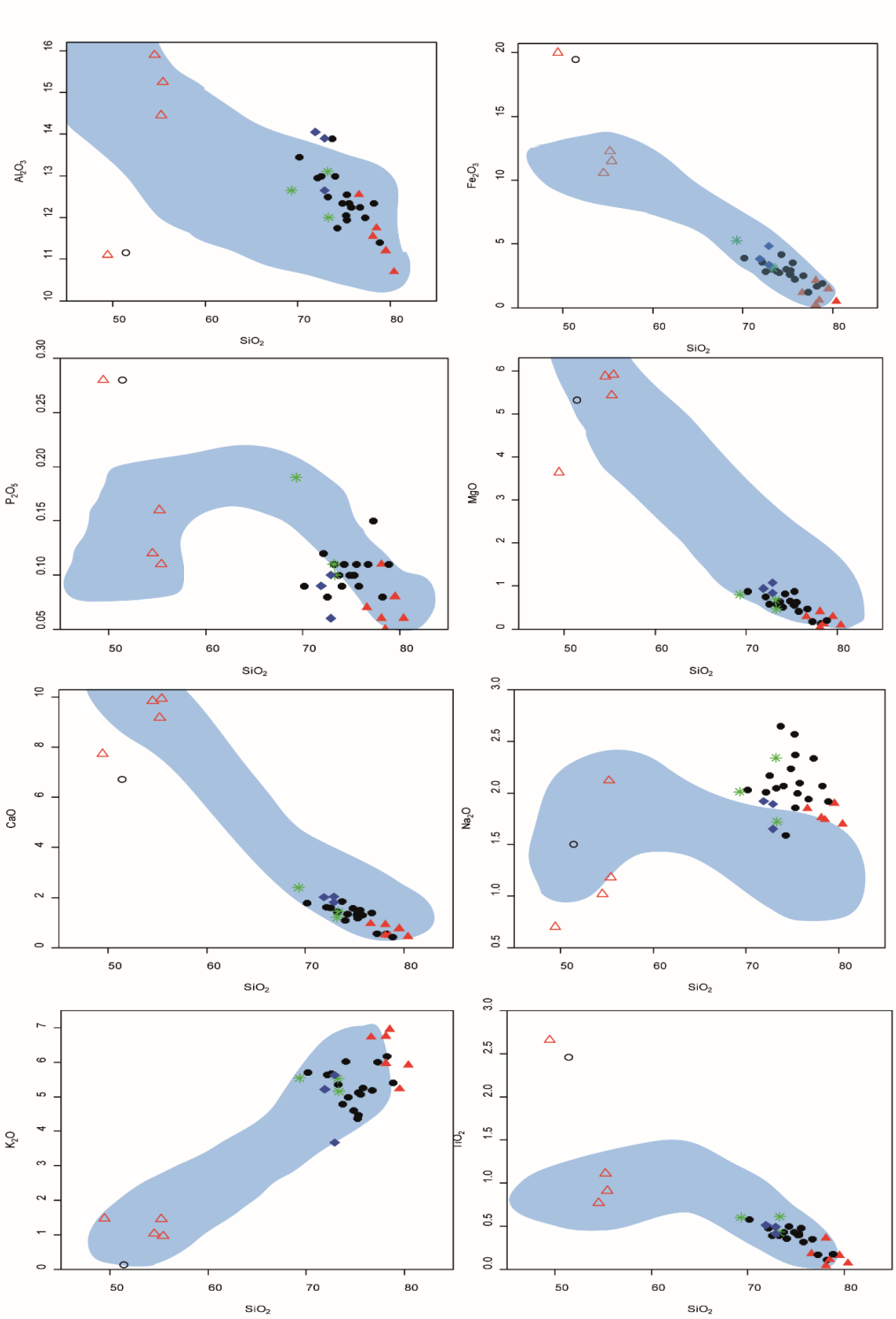


**Figure 6. Harker diagrams for the Anmatjira Orthogneiss (black circles), Aloolya Gneiss (red triangles), Possum Creek Charnockite (green stars) and the Un-named Granite (blue diamonds). With the blue fields representing data from Possum Creek Charnockite and Mylonite from the Possum Creek Charnockite (J Hopkinson 2015, pers. comm., 5 June).**

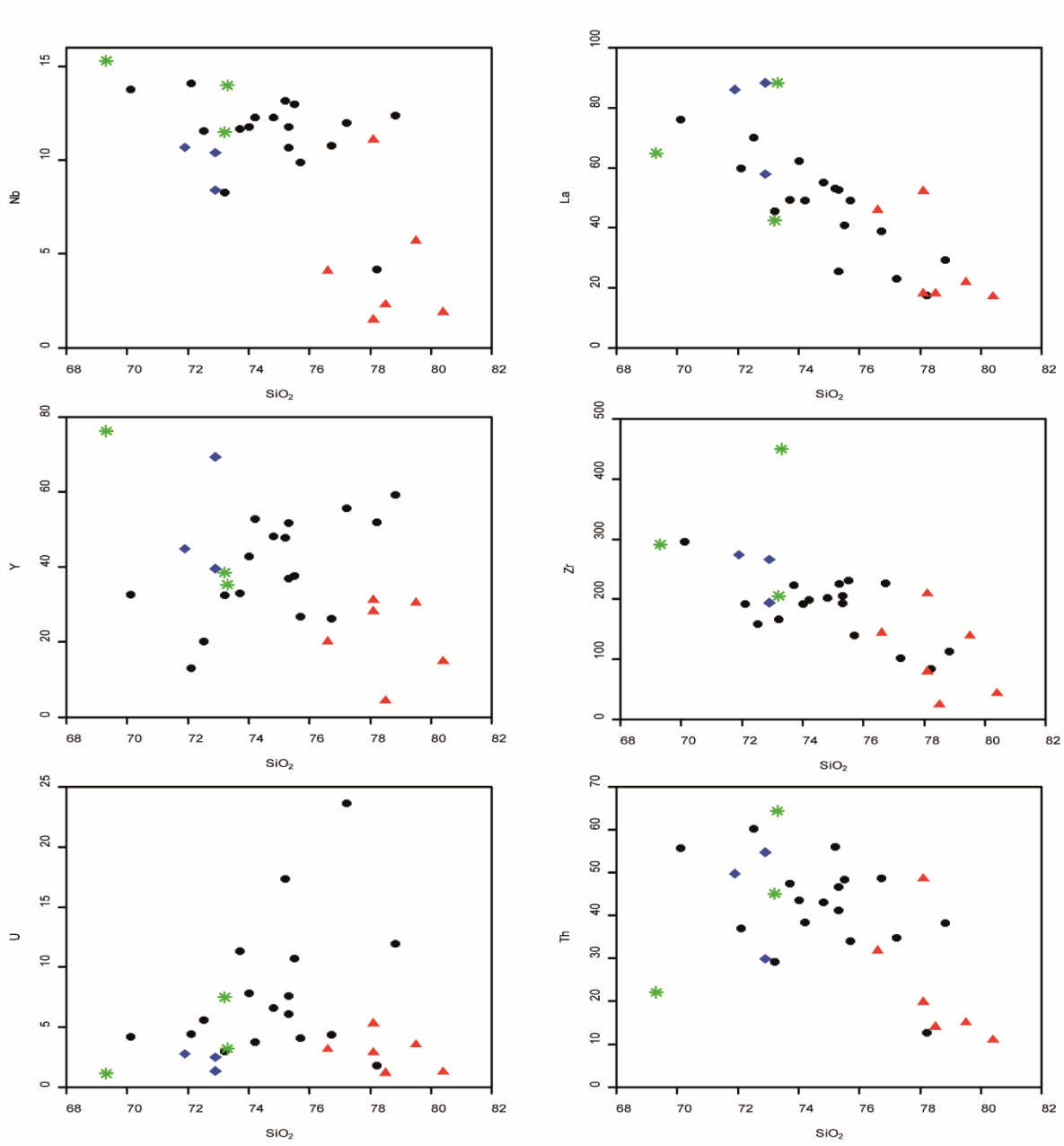


**Figure 7. Harker variation diagrams (SiO2 versus selected trace elements).**

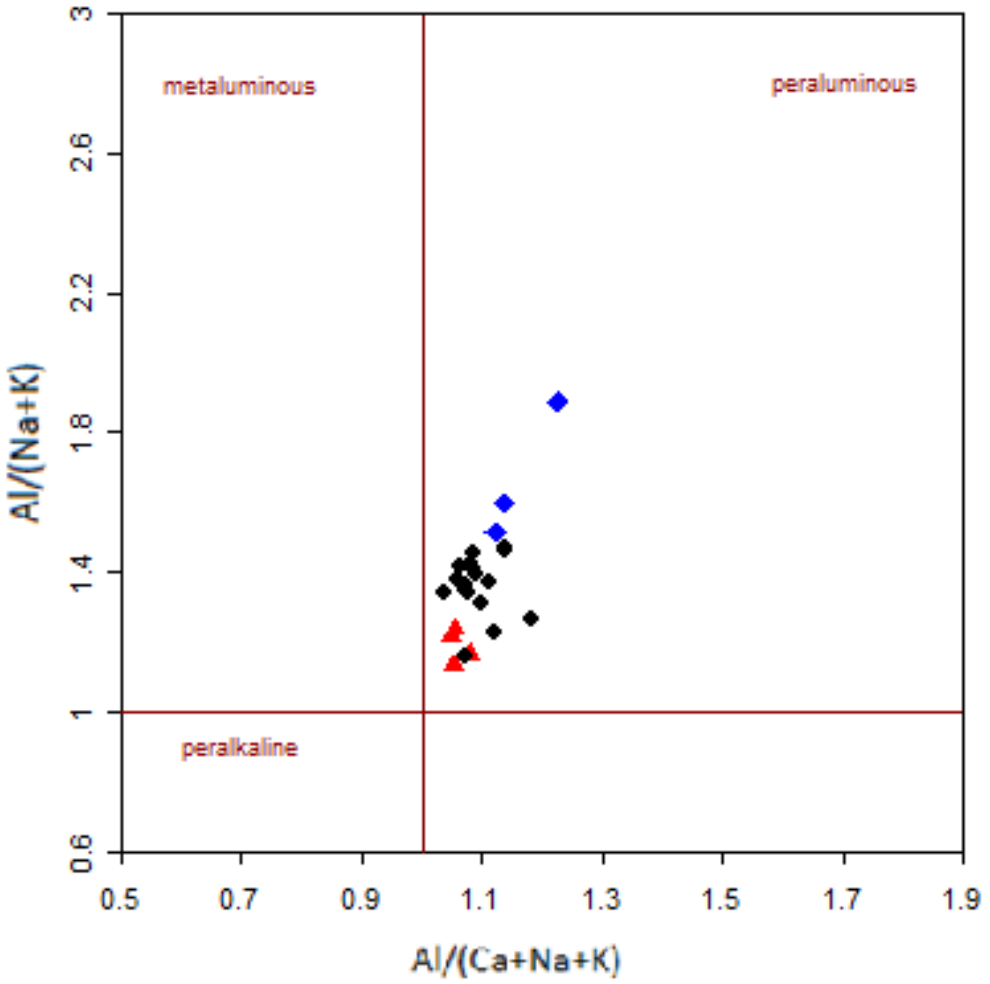


**Figure 8. Alumina Saturation Index plot for all samples from the Anmatjira Range after Frost et al (2001).**

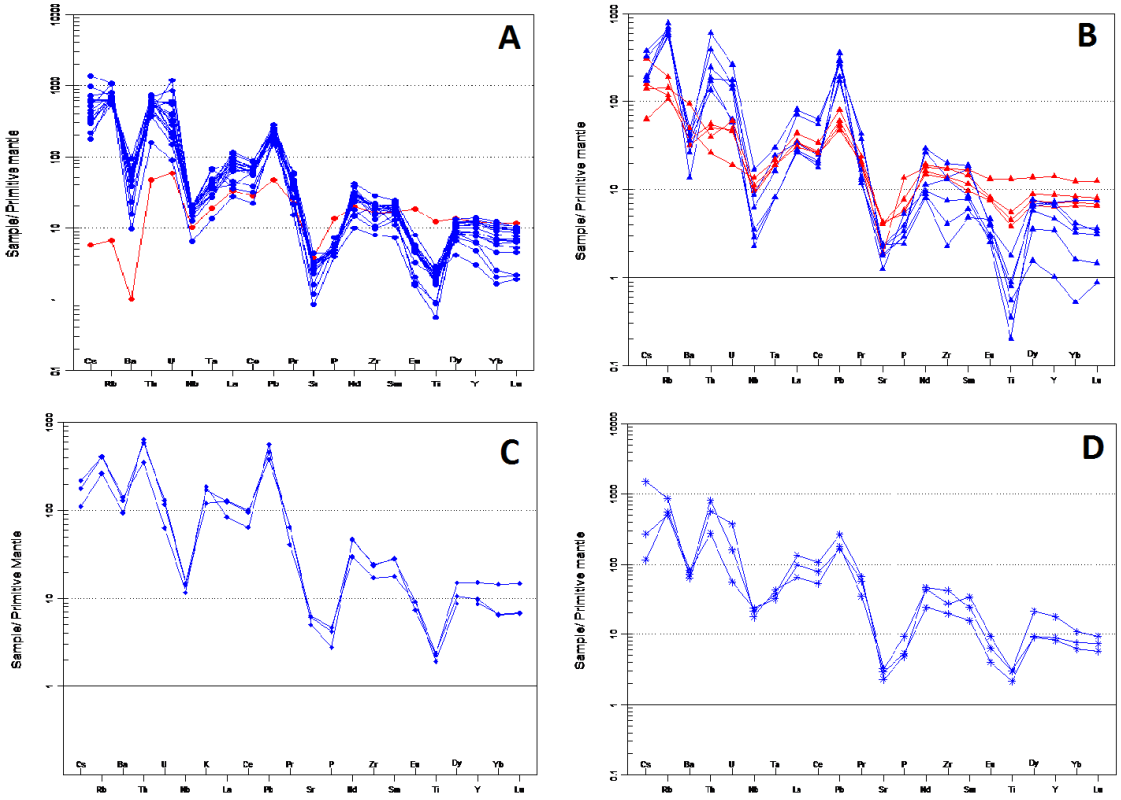


**Figure 9. Primitive mantle normalised after McDonough and Sun (1995). a) Anmatjira Orthogneiss b) Aloolya Gneiss c) Un-named Granite d) Possum Creek Charnockite. Blue lines represent granitic rocks of the Anmatjira Range while the red lines are the mafic associations**

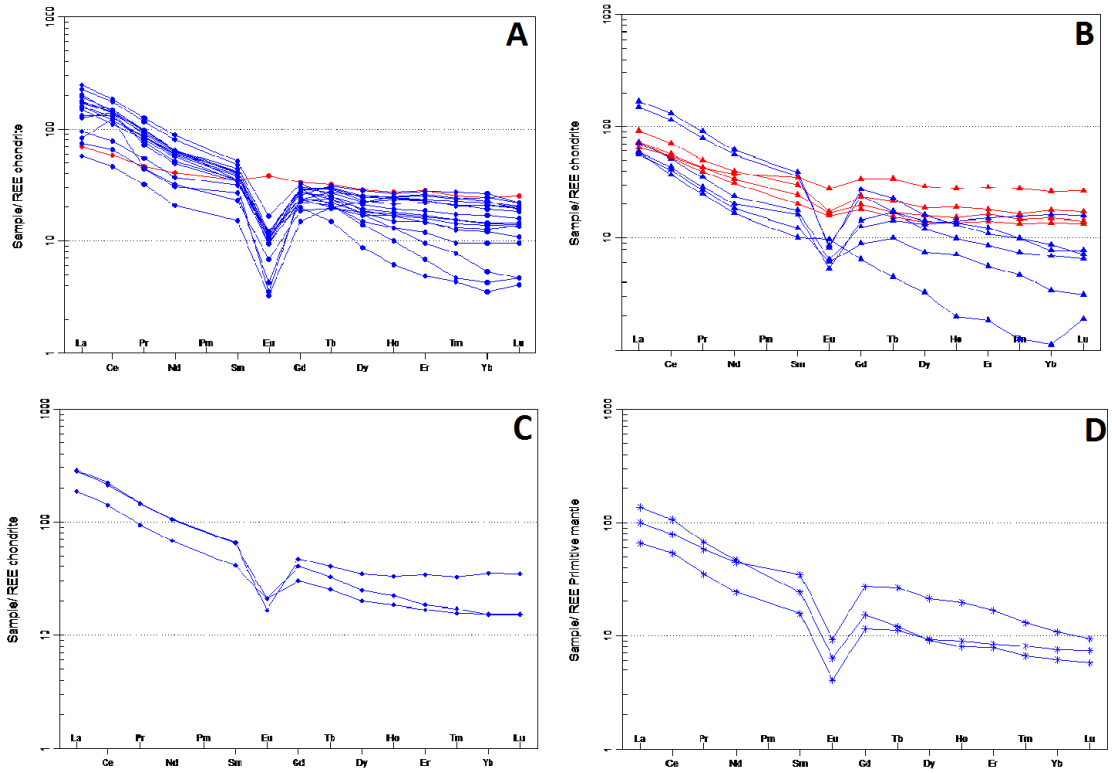


**Figure 10. REE Chondrite-normalised (Boynton 1984) a) Anmatjira Orthogneiss b) Aloolya Gneiss c) Un-named Granite d) Possum Creek Charnockite. Blue lines represent granitic rocks of the Anmatjira Range while the red lines are the mafic associations**

### 4.4 Heat Production Calculations

Surface heat production was calculated for each granitoid suite using K, U and Th readings obtained in the field with GRS, as well as geochemistry (Table 2 and 3). In locations where both GRS and whole rock geochemistry data were collected the heat production values calculated were reasonably similar. The average surface heat production calculated for the Anmatjira Orthogneiss with an age of 1984 ± 8 Ma was; 7.00 $\mu Wm^{-3}$ for whole rock geochemistry; and 6.99 $\mu Wm^{-3}$ for GRS.

The average heat production for the Aloolya Orthogneiss with an age of 1779 ± 9.8 Ma for whole rock geochemistry was 4.01 $\mu Wm^{-3}$, 0.79 $\mu W^{-3}$ for the mafic associations, and 5.84 $\mu Wm^{-3}$ for GRS data.

The average heat production for whole rock geochemistry for the Possum Creek Charnockite was 5.79 $\mu Wm^{-3}$. For the Un-named Granite with an age of 1780 ± 7.5 Ma, heat production for whole rock geochemistry was 5.15 $\mu Wm^{-3}$ and for GRS 7.63$\mu Wm^{-3}$.

**Table 2. Heat production calculations from whole rock geochemistry data**

| Sample | Rock Unit | K (wt. %) | Th (ppm) | U (ppm) | ΔTime (Ma) | Heat Production (μWm$^{-3}$) |
|---|---|---|---|---|---|---|
| Global AVG UPPER continental crust | | 2.865 | 10.3 | 2.5 | 0 | 1.69 |
| Global Avg Lower continental crust | | 1.314 | 6.6 | 0.93 | 0 | 0.85 |
| Whole crust avg | | 2.14 | 8.5 | 1.7 | 0 | 1.27 |
| AMJ-GP-01a | Anmatjira Orthogneiss | 3.97 | 47.5 | 11.4 | 1784 | 8.49 |
| AMJ-GP-01b | Anmatjira Orthogneiss | 0.1 | 3.78 | 1.15 | 1784 | 0.71 |
| AMJ-GP-02 | Anmatjira Orthogneiss | 5.129 | 12.8 | 1.8 | 1784 | 2.81 |
| AMJ-GP-03 | Anmatjira Orthogneiss | 4.457 | 29.3 | 2.98 | 1784 | 4.33 |
| AMJ-GP-04 | Aloolya Gneiss | 5.777 | 14.1 | 1.16 | 1779 | 2.84 |
| AMJ-GP-05 | Aloolya Gneiss | 5.586 | 31.8 | 3.14 | 1779 | 4.84 |
| AMJ-GP-06 | Aloolya Gneiss | 0.855 | 4 | 0.96 | 1779 | 0.84 |
| AMJ-GP-07 | Aloolya Gneiss | 0.797 | 4.44 | 0.91 | 1779 | 0.84 |
| AMJ-GP-08 | Anmatjira Orthogneiss | 3.627 | 56.2 | 17.4 | 1784 | 11.13 |
| AMJ-GP-09 | Anmatjira Orthogneiss | 5.013 | 43.6 | 7.85 | 1784 | 7.23 |
| AMJ-GP-10 | Possum Creek Charnockite | 4.59 | 45.1 | 7.48 | 1784 | 7.12 |
| AMJ-GP-12 | Aloolya Gneiss | 4.341 | 15.1 | 3.54 | 1779 | 3.39 |
| AMJ-GP-13 | Aloolya Gneiss | 4.914 | 11 | 1.25 | 1779 | 2.43 |
| AMJ-GP-14 | Aloolya Gneiss | 1.204 | 2.09 | 0.38 | 1779 | 0.57 |
| AMJ-GP-15 | Aloolya Gneiss | 1.22 | 3.18 | 1.2 | 1779 | 0.94 |
| AMJ-GP-16 | Aloolya Gneiss | 4.955 | 48.6 | 5.3 | 1779 | 6.73 |
| AMJ-GP-17 | Anmatjira Orthogneiss | 4.739 | 55.8 | 4.22 | 1784 | 6.87 |
| AMJ-GP-18 | Possum Creek Charnockite | 4.598 | 22.1 | 1.13 | 1774 | 3.17 |
| AMJ-GP-19 | Aloolya Gneiss | 5.611 | 19.9 | 2.87 | 1779 | 3.83 |
| AMJ-GP-20 | Possum Creek Charnockite | 4.283 | 64.4 | 3.21 | 1774 | 7.07 |

| | | | | | | |
|---|---|---|---|---|---|---|
| AMJ-GP-21 | Anmatjira Orthogneiss | 4.714 | 60.3 | 5.61 | 1784 | 7.69 |
| AMJ-GP-22 | Anmatjira Orthogneiss | 4.69 | 37.1 | 4.44 | 1784 | 5.49 |
| AMJ-GP-23 | Anmatjira Orthogneiss | 4.142 | 38.5 | 3.75 | 1784 | 5.23 |
| AMJ-GP-24 | Anmatjira Orthogneiss | 4.366 | 34.1 | 4.09 | 1784 | 5.06 |
| AMJ-GP-25 | Anmatjira Orthogneiss | 4.316 | 48.8 | 4.4 | 1784 | 6.29 |
| AMJ-GP-27 | Anmatjira Orthogneiss | 4.499 | 38.3 | 12 | 1784 | 8.10 |
| AMJ-GP-29 | Anmatjira Orthogneiss | 4.997 | 34.9 | 23.7 | 1784 | 11.97 |
| AMJ-GP-30 | Anmatjira Orthogneiss | 3.71 | 46.7 | 6.12 | 1784 | 6.57 |
| AMJ-GP-31 | Anmatjira Orthogneiss | 3.826 | 43.2 | 6.6 | 1784 | 6.49 |
| AMJ-GP-32 | Anmatjira Orthogneiss | 4.258 | 41.3 | 7.61 | 1784 | 6.79 |
| AMJ-GP-33 | Anmatjira Orthogneiss | 4.208 | 48.5 | 10.8 | 1784 | 8.41 |
| AMJ-GP-34 | Un-named Granite | 3.046 | 54.8 | 2.47 | 1780 | 5.79 |
| AMJ-GP-35 | Un-named Granite | 4.333 | 49.8 | 2.75 | 1780 | 5.80 |
| AMJ-GP-36 | Un-named Granite | 4.673 | 29.9 | 1.34 | 1780 | 3.87 |
| CAT Group | | 3.41 | 21.84 | 3.61 | 1770-1750 | 3.57 |
| Main Group | | 4.32 | 29.08 | 4.68 | 1820-1750 | 4.69 |
| HHP Group | | 12.75 | 71.98 | 5.35 | 1730-1710 | 11.29 |

**Table 3. Heat production calculations from gamma ray spectrometer data. m= megacrystic outcrop, f = fine grained outcrop**

| Sample | Rock Unit | K (wt. %) | Th (ppm) | U (ppm) | ΔTime (Ma) | Outcrop | Heat Production ($\mu Wm^{-3}$) |
|---|---|---|---|---|---|---|---|
| Global AVG UPPER continental crust | | 2.865 | 10.3 | 2.5 | 0 | | 1.69 |
| Global Avg Lower continental crust | | 1.314 | 6.6 | 0.93 | 0 | | 0.85 |
| Whole crust avg | | 2.14 | 8.5 | 1.7 | 0 | | 1.27 |
| AMJ-GP-02 | Anmatjira Orthogneiss | 3.951 | 15.6 | 3.76 | 1784 | f | 3.42 |
| AMJ-GP-03 | Anmatjira Orthogneiss | 3.76 | 37.63 | 6.03 | 1784 | m | 5.86 |
| AMJ-GP-04 | Aloolya Gneiss | 4.499 | 28.1 | 6 | 1779 | f | 5.28 |
| AMJ-GP-08 | Aloolya Gneiss | 4.20 | 60.22 | 13.22 | 1784 | m | 10.16 |
| AMJ-GP-12 | Aloolya Gneiss | 3.80 | 28.75 | 5.15 | 1779 | m | 4.87 |
| AMJ-GP-16 | Aloolya Gneiss | 3.89 | 53.25 | 6.87 | 1779 | m | 7.37 |
| AMJ-GP-17 | Anmatjira Orthogneiss | 4.14 | 64.64 | 7.48 | 1784 | m | 8.52 |
| AMJ-GP-34 | Un-named Granite | 3.90 | 47.71 | 8.87 | 1780 | m | 7.63 |

**Table 4. Average heat production of GRS versus whole rock geochemistry**

| Granite | Age | Average GRS Heat Production | Average Whole Rock Geochemistry |
|---|---|---|---|
| Anmatjira Orthogneiss | 1784 | 6.99 | 7.00 |
| Aloolya Gneiss | 1779 | 5.84 | 4.01 |
| Un-named Granite | 1780 | 7.63 | 5.15 |
| Possum Creek Charnockite | 1774 | - | 5.79 |

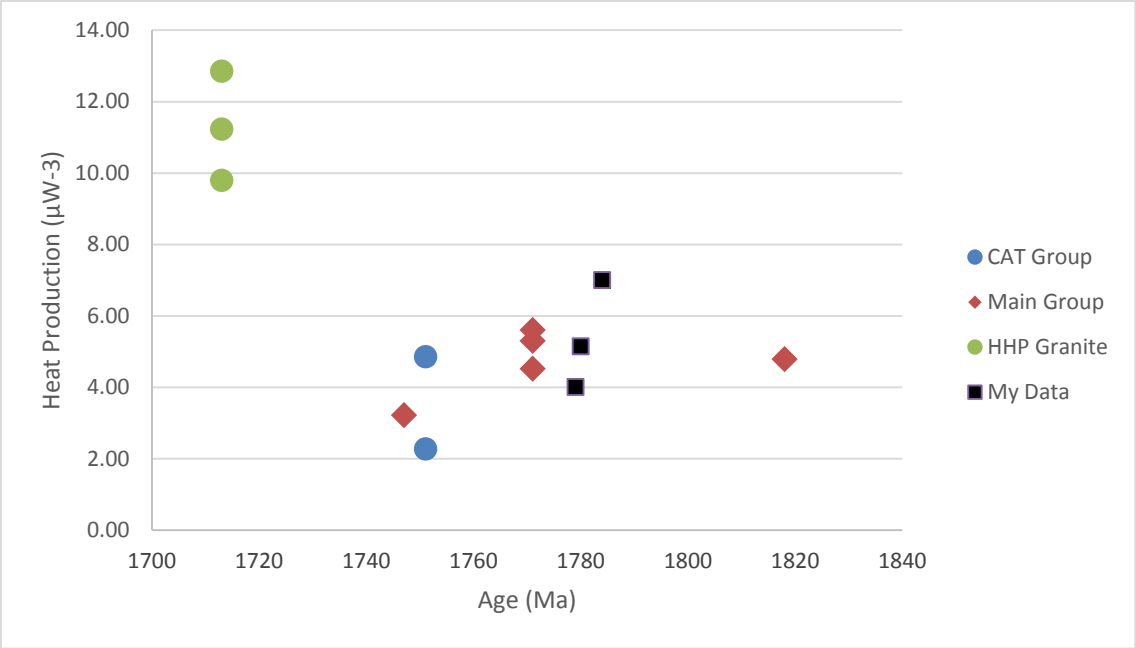


**Figure 11. Average heat production from Zhao's (1995) Cat Group, Main Group and HHP Group as well as heat production of granites from this study**

### 4.5 Sm-Nd Isotopes

Results from Sm-Nd isotopic analyses are summarised in Table 5. The εNd (T) was calculated for each sample from the ages determined via U-Pb geochronology summarised in Table 1. Samples, AMJ-GP-01a, AMJ-GP-05, AMJ-GP-19, AMJ-GP-24 and AMJ-GP-36 have relatively evolved εNd values between -3.3 to -4.4. Sample AMJ-GP-01b, the mafic association of the Anmatjira Orthogneiss has a slightly less evolved εNd value of -3.5.

**Table 5. Sm-Nd isotope data for selected samples from the Anmatjira Range.**

| Sample | Rock Unit | $^{147}Sm/^{144}Nd$ | $^{143}Nd/^{144}Nd$ | εNd (T) | Age |
|---|---|---|---|---|---|
| AMJ-GP-01a | Anmatjira Orthogneiss | 0.1219 | 0.510097 | -4.6 | 1784 |
| AMJ-GP-01b | Anmatjira Orthogneiss | 0.1756 | 0.510154 | -3.5 | 1784 |
| AMJ-GP-05 | Aloolya Gneiss | 0.1290 | 0.510120 | -4.3 | 1779 |
| AMJ-GP-19 | Aloolya Gneiss | 0.1527 | 0.510158 | -3.5 | 1779 |
| AMJ-GP-24 | Anmatjira Orthogneiss | 0.1277 | 0.510133 | -3.9 | 1784 |
| AMJ-GP-36 | Un-named Granite | 0.1197 | 0.510114 | -4.4 | 1779 |

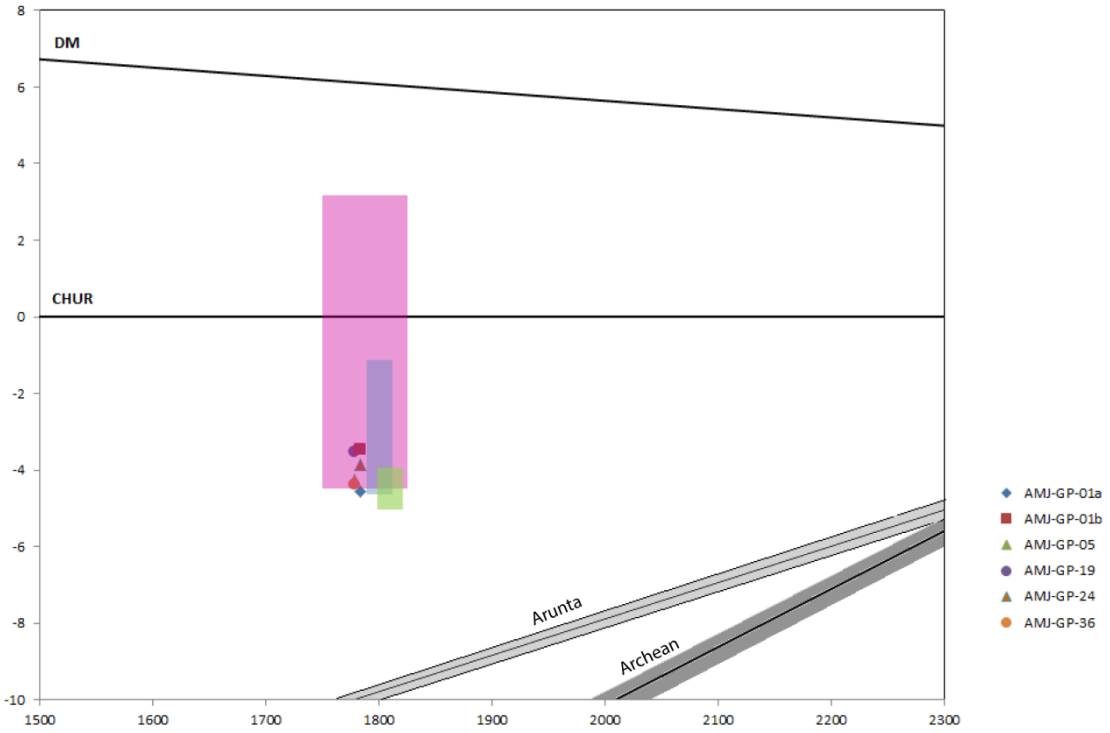


**Figure 12. εNd vs time for granitoid samples from the Anmatjira Range compared with data from J Hopkinson (2015, pers. comm., 1 July) (blue field), W Lau (2015, pers. Comm., 8 September) (green field), and data from Hoatson et al, 2005 and STIKR NTGS, (Pink Field).**

### 4.6 Inherited Zircon Ages

Figure 13 shows the age of inherited zircons from the granites compared to detrital zircons from the Lander Rock Formation. The dominant inherited age peak from the granites is slightly younger than that of the Lander Rock Formation. This could be due to differences in sample size or metamorphic overprinting which has occurred in the Anmatjira Range. The older peaks for inherited zircons from the granites match better with the peaks of detrital zircons from the Lander Rock Formation.

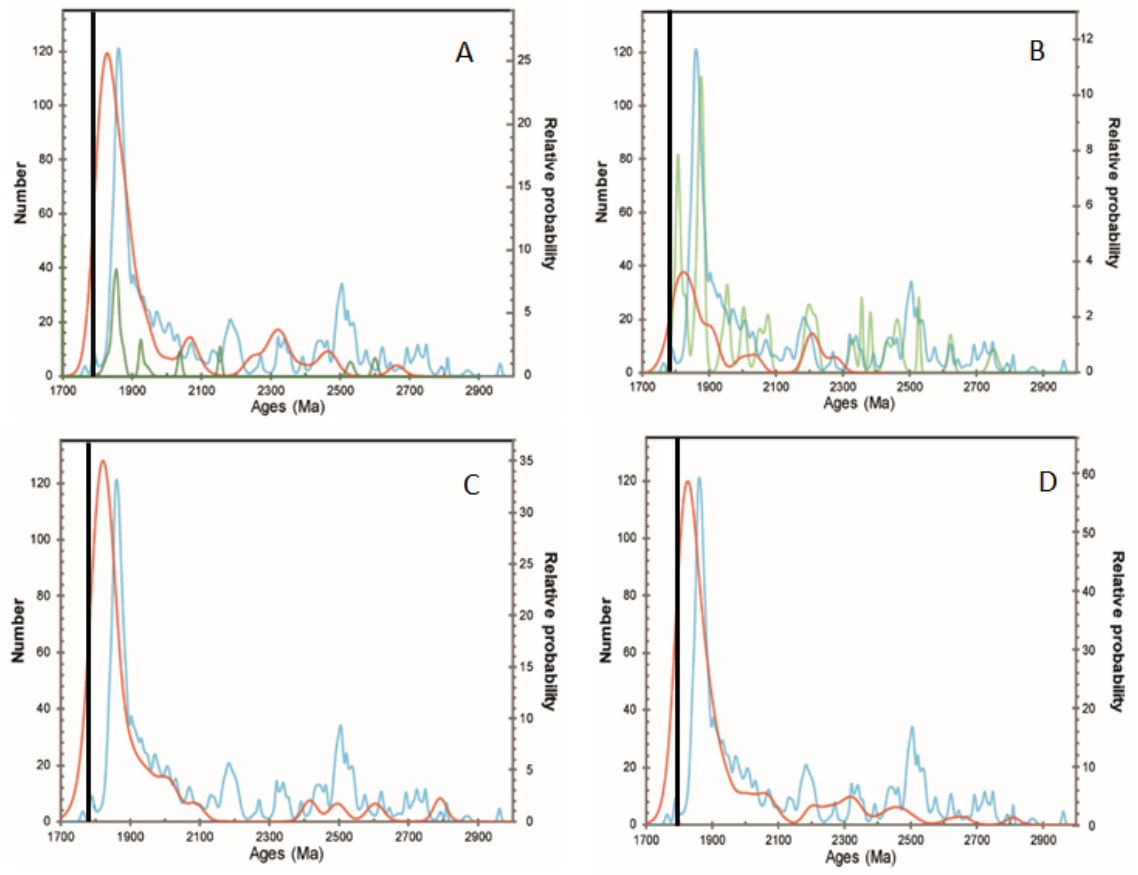


**Figure 13. Probability density plots, comparing published 207Pb/206Pb ages for the Lander Formation (Claoue-Long et al, 2008, Claoue-Long 2008, Vry et al, 1996) with zircon ages from samples collected as well as published ages (Worden KE et al, 2008). a) Anmatjira Orthogneiss (red), Anmatjira Orthogneiss published data (green), Lander Formation (blue), b) Aloolya Gneiss (red), Aloolya Gneiss published data (green), Lander Formation (blue), c) Un-named Granite (red), Lander Formation (blue), d) all combined granites samples (red), Lander Formation (blue). The black line represents the magmatic age**

# 5. DISCUSSION

## 5.1 Geochronology of the Anmatjira Range

### 5.1.1 AGE OF FELSIC AND MAFIC ROCKS AND MAGMATIC EVOLUTION

The U-Pb zircon crystallisation ages provide important data to unravel the magmatic history of the Paleoproterozoic Anmatjira Range. The ages determined from this study, when combined with previous studies (Scrimgeour IR, 2013, Hand et al., 1995, Hoatson et al, 2005), illustrates that the granitic (Anmatjira, Aloolya and Un-named Granite),

felsic and mafic rocks in the Anmatjira Range were emplaced during the Paleoproterozoic. The U-Pb ages from this study for all three granitic rocks (Anmatjira Orthogneiss 1784 ± 6.6 Ma, Un-named Granite 1780 ± 7.5 Ma and Aloolya Gneiss 1779 ± 9.8 Ma) are within error of each other. Combined with field observations including that the Aloolya Gneiss intrudes the Anmatjira Orthogneiss, which is believed to still have been molten at the time of intrusion (Scrimgeour IR, 2013), indicates that they all formed during a single magmatic event. The Tyson Creek Granulite has a U-Pb age of 1767 ± 14 Ma (Hand et al., 1995) and the Possum Creek Charnockite 1774 ± 6 Ma and 1767 ± 14 Ma (Hand et al., 1995, Collins and Williams, 1995). Hence the mafic rocks of the Anmatjira Range are within error of the granitic rocks and could all be a part of the same magmatic event. As all the granites in this study are from a singular magmatic event then it would be expected that they all have the same source.

### 5.1.2 DIFFICULTY OF THE ANMATJIRA RANGE ZIRCON DATING

The U-Pb ages determined from this study have been compared with previously published ages from the NTGS, GSA and Scrimgeour (2013) and are all within error of each other. However there are some complications when processing and interpreting geochronological data. Many of the zircons that were imaged using CL exhibited: metamorphic and igneous overgrowth, inherited cores, and metamictization which related to the abundance of radioactive elements in the zircon (Hanchar and Miller, 1993, Deliens et al., 1977). Many zircons displayed a distinct core rim relationship. In cases where the core was higher in U than the rim, the core would often experience differential metamicitzation. This eventually resulted in the expansion of the U rich core and ended in fracturing of the rim (Corfu et al., 2003). From CL images it is clear that many of the zircons contained inherited cores as magmatic zoning. It is possible that

during an analysis the laser ablating can collect data from more than one growth zone, resulting in unrepresentative or discordant ages. In this study many of the zircons also exhibited metamorphic overprinting. This could result in analyses becoming discordant as more than one growth zone would often be hit. The ages that were collected from areas of metamorphic overprinting often coincided with the ages of thermal metamorphic events that have were experienced in the Anmatjira Range. Analyses that presented ages corresponding with a thermal metamorphic event were discarded from the analyses for a magmatic age. In the adjacent Reynold Ranges it has been noted that metamorphic overgrowth of zircons occurred when temperatures in excess of 700 °C were reached (Rubatto et al., 2001). It is reasonable to extrapolate that these conditions are the same for the Anmatjira Range. As many of the metamorphic events experienced in the Aileron Province had been described as high temperature and low pressure (Hand and Buick, 2001), it is it can be assumed that metamorphic overprinting would affect many of the zircons in this study.

### 5.2 Geochemistry of the Granites of the Anmatjira Range

The HHP granites from this study are mainly felsic rocks (>70 wt% $SiO_2$) with all the associations being mafic (<60 wt% $SiO_2$). The Aloolya Gneiss is the most fractionated of the granites (Figure 7) and also has the lowest average heat production from both GRS and whole rock geochemistry (Table 4). A decrease in Th with increasing fractionation, results in the most fractionated being the least heat producing (the Aloolya Gneiss) (Figure 8). This decrease in Th could be due to the early crystallising phosphate minerals such as monazite, which removes U, Th and REE from the melt.

White and Chappell (1977), proposed that the geochemistry of granitoids reflects the geochemistry of their source rock. Rocks that have an Al value which is greater than the combined values of K, Na and Ca are said to be peraluminous. Peraluminous granites are most likely the result of melting of a metasedimentary material (Garcia et al, 1994). As the majority of granites in the Anmatjira Range plot as peraluminous this suggests that they melted part of a metasedimentary package of the Anmatjira Range.

There is notable variation in REE within a single suite which can be attributed to the differing contributions of crustal and mantle melt of each sample. The felsic granitic samples as well as the charnockite samples all show negative Eu anomalies. Samples of mafic associations show much less negative or slightly positive Eu anomalies. These results indicate that plagioclase was a restitic phase during crustal melting and granite production.

Negative Eu anomalies indicate that these granitic samples have a crustal source where there is plagioclase in the residue. Further evidence for plagioclase being left behind in the residue is the depletion of Sr, Ba and En compared to the other REE in the depleted mantle spider plot (Figure 10). The decrease of both $Al_2O_3$ and CaO with increasing $SiO_2$, further supports fractionation of plagioclase. It would therefore be expected that there would be a concentration of plagioclase in the lower crust.

The HREE elements have a flat trend, which signifies that garnet was not left behind in the residue.

All three granites from the Anmatjira Range present similar trends in their geochemistry. The Harker diagrams show similar trends with increasing $SiO_2$ and the REE trends and the spider diagrams are similar. It is proposed that the three granites from the Anmatjira Range are co-magmatic.

Further evidence for these granites being co-magmatic is that the U-Pb ages of all the granites analysed in this study are within error.

Based on the geochemistry, discrimination diagrams and Nd isotope data a crustal or metasedimentary source is inferred for the granitic and charnockite samples, while a more mantle derived source is inferred for the mafic associations.

In the S-E of the Anmatjira Range is a coarse porphyritic garnet-bearing granitic, augen gneiss. This suite was previously assigned as the Un-name granite. It is possible that this granite is its own suite or belongs to one of the other suites in the Ranges, as all three granites (Anmatjira Orthogneiss, Aloolya Gneiss and the Un-named Granite) came from a singular magmatic event.

As mentioned above, the U-Pb ages of all the granites analysed in this study are within error, demonstrating that they are co-magmatic. They have a field relationship which suggests that the Anmatjira Orthogneiss was still partially molten when it was intruded by the younger Aloolya Gneiss (Scrimgeour IR, 2013). As the geochemistry of all three granitic rocks are similar it is appropriate to assume that they all share the same source. All of the spider diagrams highlight that for the majority of samples there is a negative Eu anomaly indicating a large crustal influence. However for both the Anmatjira Orthogneiss and the Aloolya Gneiss some samples have a notably less negative Eu anomaly, because they are the mafic associations. This all suggests a strong influence from the continental crust within these granites, however, there is still a mafic component which could have supplied both heat and source material to the region.

## 5.3 Heat Production of the Anmatjira Range

### 5.3.1 VARIATION IN HEAT PRODUCTION

As noted in the sample and petrography section, the Anmatjira Orthogneiss, Aloolya Gneiss and the Possum Creek Charnockite have megacrystic and fine grained variations. The two types of outcrops also resulted in a variation in heat production (Table 2 & 3). In the granitic samples (Anmatjira Orthogneiss and Aloolya Gneiss), heat production is higher in the megacrystic samples, compared to the finer grained outcrops. The opposite relationship is observed in the Possum Creek Charnockite, where the finer grained outcrops resulted in higher heat production when compared to coarser grained outcrops. The fine granitic samples are less enriched in U and Th as they are formed from the residual melt. During crystallisation of the magma most of the Th would preferentially go into monazite, therefore concentrating in the megacrystic variation.

### 5.3.2 GRS VS. WHOLE ROCK GEOCHEMISTRY

Two methods were used to calculate heat production: GRS in the field, and whole rock geochemistry. There was some difference between the results obtained using the two methods (Table 4).The variation for the Anmatjira Orthogneiss was minimal and likely due to difference in the collection of HPE abundances. However, for the Aloolya Gneiss and the Un-named Granite there was a notable variation between results obtained from the GRS data and whole rock geochemistry methodology. In the field it was observed that the Aloolya Gneiss and the Un-named Granite were both extremely weathered. This may explain why the GRS heat production was notably higher than the whole rock geochemistry average. As only the surface was weathered, the sample area of the GRS would reach areas of the outcrop which were unaffected by weathering and consequent

loss of HPE, resulting in a higher heat production. The average loss of radioactive elements is ~20-30% for weathered rocks; however they are many factors which could affect this percentage (Dickson & Scott, 1997).

### 5.4 Sources of High Heat Producing Granites

In this study all samples both mafic and felsic yielded negative εNd values (Figure 13), illustrating a large evolved crustal influence. There is no significant difference for εNd between the felsic and mafic samples or between the three granite suites of the Anmatjira Range. εNd data from J Hopkinson (2015, pers.comm.,1July), W Lau (2015 pers. comm., 8 September), Hoatson et al (2005) and STRIKE (Northern Territory Geological Survey), range from more negative εNd to positive values. This variation in εNd values suggests that the parent magma would have been a mix of both the pre-existing crust and also some juvenile mantle derived magma.

It has been proposed by McLaren and Powell (2014), that granites of the Proterozoic Australia first underwent the addition of a juvenile mafic source into the lower crust. This was followed by melting of the lower and upper crust with the heat from the mafic source assisting in this melting. This could account for the mafic influence which in observed in granite suites across the Arunta Inlier (Figure 13).

As mentioned above, εNd values of the samples in this study suggest an evolved crustal source of the granites. This, combined with the knowledge that the granites are peraluminous, strongly implies the source rock was an enriched metasedimentary unit. The dominant age populations of zircons from the Lander Rock Formation are between 1880 – 1840 Ma. U-Pb ages from previous studies of this Formation (Claoue-Long et al., 2008a,Claoue-Long et al., 2008b, Vry et al., 1996), were compared to ages for the

granitic rocks of the Anmatjira Range from both this and previous studies (Worden KE et al, 2008) (Figure 13).

Figure 6a shows that the published data of inherited zircons from the Anmatjira Orthogneiss is almost an exact match to the U-Pb detrital ages of the Lander Rock Formation, whereas the U-Pb ages determined from this study are slightly younger. The results are very similar for the Aloolya Gneiss, however the published U-Pb ages for the Aloolya Gneiss are slightly older than the Lander Rock Formation detrital zircon ages. The U-Pb ages of inherited zircons from the study are again slightly younger than the peak ages of the Lander Rock Formation. A reason for these variations could include that the sample size of the Lander Rock Formation is much larger than that of the granites samples, as well as difference in the sample size. When all the granitic U-Pb ages were combined from the three samples the peak age was 1832 Ma compared to a peak of 1865 Ma from the Lander Rock Formation.

In the field it is was observed that the granites intrude the Lander Rock Formation (Scrimgeour, 2013). This relationship means that the Lander Rock Formation cannot be the source rock. Instead a metasedimentary package that is older but similar to the Lander Rock Formation is the most likely source for the granites.

There is a wide range of inherited peak ages as well as detrital zircons; it is possible that one of the older peaks is that of the unexposed source rock. This source rock would be older than the Lander Rock Formation but would share similarities to the geochemical trends which are presented in this study.

Whole Rock Geochemistry from OZCHEM (Budd AR et al., 2000) of the Lander Rock Formation shows that it is enriched in U, Th and K when compared to average levels of the upper continental crust (Taylor and McClennan, 1985, Wedepohl, 1995). With an

enrichment of HPE the Lander Rock Formation has high heat production for a metasediment of 4.01 $\mu W^{-3}$. This however isn't sufficiently enriched to explain the extraordinary enrichments of the granites, there must have been another source which was being added. Possibly an enriched mafic source as suggested by the εNd.
There is a variation between both the individual granites, and the difference in peak population between the granites and the Lander Rock Formation. However the age of inherited zircons, when combined with evidence from εNd values and heat production values, suggest that a metasedimentary unit similar to the Lander Rock Formation is the most likely source of the HHP granites of the Anmatjira Range.

## 6. CONCLUSIONS

The Paleoproterozoic granites of the Anmatjira Range, which range in age from 1784 to 1779 Ma, are all extraordinarily enriched in U and Th, resulting in them being high heat producing. Heat production varied slightly between granites, and also between megacrystic and fine grained variations. As the U-Pb magmatic ages of these granitic suites are all within error of each other and have no significant difference between their εNd values, it can be concluded that they share a common source. Similar to the geochronology there is little difference in heat production values between the three granite suites, with all considered to be high heat producing. There are some variation in heat production values between whole rock geochemistry and GRS. This however, can be attributed to the effect of weathering on the concentration of HPE. From the negative εNd values ranging from -3.5 to -4.6, and other published results which are more positive, it can be concluded that granites were derived from an evolved crustal source which has mixed with some mantle-derived material. With most samples plotting in the peraluminous field it can be concluded that the source for these granites was a

metasedimentary rock. Within the Anmatjira Range the Lander Rock Formation is a metasedimentary package with a dominant age of 1840-1880 Ma. The inherited U-Pb ages of this study and previous works compared well with the dominant detrital age populations of the Lander Rock Formation. From all the evidence presented in this study, the most likely source of the highly enriched granites of the Anmatjira Range is a unit similar to, but older than, the Lander Rock Formation in combination with some juvenile mafic material.

## ACKNOWLEDGMENTS

I would like to thank Karin Barovich for her excellent guidance, support and encouragement throughout this year. Martin Hand, Justin Payne and Kieran Meaney are also thanked for their invaluable input and assistance. Aoife McFadden and Adelaide Microscopy are thanked for their assistance with SEM imaging and LA-ICP-MS analysis. James Hopkinson and WingKei Lau are thanked for their assistance in the field as well as their support. David Bruce is thanked for his assistance in the isotope lab. Katie Howard is thanked for her patience and guidance throughout the year.

## REFERENCES

ANDERSON, J. R., KELSEY, D. E., HAND, M. & COLLINS, W. J. 2013. Conductively driven, high-thermal, gradient metamorphism in the Anmatjira Range, Arunta region, central Australia. Journal of Metamorphic Geology, 31, 1003-1026.

BEA, F. 1996. Residence of REE, Y, Th and U in Granites and Crustal Protoliths; Implications for the Chemistry of Crustal Melts. Journal of Petrology, 57, 521 - 552.

BEA, F. 2012. The sources of energy for crustal melting and the geochemistry of heat-producing elements. Lithos, 153, 278-291.

BUDD, A.R., HAZEL, M.S., SEDGMEN, A., SEDGMEN, L., WYBORN, L.A.I. & RYBURN, R., 2000. OZCHEM dataset release 1 documentation: AGSO's national whole rock geochemistry database. Record 2000/012. Australian Geological Survey Organisation, Canberra

CAWOOD, P. A. & KORSCH, R. J. 2008. Assembling Australia: Proterozoic building of a continent. Precambrian Research, 166, 1-35.

CLAOUE-LONG, J., EDGOOSE, C. & WORDEN, K. 2008a. A correlation of Aileron Province stratigraphy in central Australia. Precambrian Res., 166, 230-245.

CLAOUE-LONG, J., MAIDMENT, D., HUSSEY, K. & HUSTON, D. 2008b. The duration of the Strangways Event in central Australia: Evidence for prolonged deep crust processes. Precambrian Res., 166, 246-262.

COLLINS, W.J., AND SHAW, R.D., 1995, Geochronological constraints on orogenic event in the Arunta Inlier – a review: Precambrian Research., 71, 315-346

COLLINS, W. & WILLIAMS, I. S. 1995. SHRIMP ionprobe dating of short-lived Proterozoic tectonic cycles in the northern Arunta Inlier, central Australia. Precambrian Res., 71, 69-89.

CORFU, F., HANCHAR, J. M., HOSKING, P. W. W. & KINNY, P. D. 2003. Atlas of zircon texture. Reviews in Mineralogy and Geochemistry 53, 469-500.

DELIENS, M., DELHAL, J. & TARTE, P. 1977. Metamictization and U-Pb systematics - a study by infrared absorption spectrometry of precambrian zircons. Earth and Planetary Science Letters, 33, 331- 344.

DICKSON, B.L., SCOTT, K.M. 1997. Interpretation of aerial gamma-ray survey – adding the geochemical factors. AGSO Journal of Australian Geology and Geophysics 17, 187-200.

GATCIA, D., FONTEILLES, M. & MOUTTE J. Sedimentary Fractionations between Al, Ti and Zr and the Genesis of Strongly Peraluminous Granites. The Journal of Geology 102, 411-422

HANCHAR, J.M. & MILLER, C.F. 1993. Zircon zonation patterns as revealed by cathodoluminescence and backscatterd electron images: Implication for interpretation of complex crustal histories. Chemical Geology, 110, 1-13.

HAND, M. & BUICK, I. S. 2001. Tectonic evolution of the Reynolds-Anmatjira Ranges: a case study in terrain reworking from the Arunta Inlier, central Australia. Geological Society Special Publication, 184, 237-260.

HAND, M., FANNING, M. & SANDIFORD, M. 1995. Low-P high-T metamorphism and the role of high-heat producing granites in the northern Arunta Inlier. Abstracts - Geological Society of Australia, 40, 60-61.

HOATSON, D.M., SUN, S., CLAOUE-LONG, J.C. 2005a. Proterozoic mafic-ultramafic intrusions in the Arunta Region, central Australia Part 1: Geological setting and mineral potential. Precambrian Research. 142, 93-133.

HOATSON, D.M., SUN, S., CLAOUE-LONG, J.C. 2005b. Proterozoic mafic-ultramafic intrusions in the Arunta Region, central Australia Part 2: Event chronology and regional correlations. Precambrian Research. 142, 134-158.

KROMKHUN K. 2010 Petrogenesis of high heat producing granite: implication for Mt Painter Province, South Australia. School of Earth and Environmental Science. University of Adelaide: University of Adelaide.

MARSHALL V. 2013 Petrological, geochemical and geochronological charcterisation of heat-producing granites. School of Earth Sciences. Queensland: The University of Queensland.

MCLAREN, S. & POWEL, R. 2014. Magmatism, orogeny and the origin of high-heat-producing granites in Australian Proterozoic terranes. J. Geol. Soc., 171, 149-152.

PAYNE J. L., BAROVICH K. M. & HAND M. 2006 Provenance of metasedimentary rocks in the northern Gawler Craton, Australia: Implications for Palaeoproterozoic reconstructions, Precambrian Research, vol. 148, no. 3, pp. 275-291.

RÖSEL, D., ZACK, T. & BOGER, S. D. 2014. LA-ICP-MS U–Pb dating of detrital rutile and zircon from the Reynolds Range: A window into the Palaeoproterozoic tectonosedimentary evolution of the North Australian Craton. Precambrian Research, 255, 381-400.

RUBATTO, D., WILLIAMS, I. S. & BUICK, I. S. 2001. Zircon and monazite response to prograde metamorphism in the Reynolds Range, central Australia. Contributions to Mineralogy and Petrology, 140, 458-468.

SANDIFORD, M., MCLAREN, S., & NEUMANN, N. 2002. Long-term thermal consequences of the redistribution of heat-producing elements associated with large-scale granitic complexes. Journal of Metamorphic Geology, 20, 87-98.

SHAE, R.D., WELLMAN, P., GUNN, P., WHAITAKER, A.J., TARLOWSKI, C., MORSE, M.P., 1995. Australian crustal elements map: geological model for the tectonic framework of the continent. AGSO Research Newsletter 23, 1-3.

SLÁMA, J., KOŠLER, J., CONDON, D. J., CROWLEY, J. L., GERDES, A., HANCHAR, J. M., HORSTWOOD, M. S. A., MORRIS, G. A., NASDALA, L., NORBERG, N., SCHALTEGGER, U., SCHOENE, B., TUBRETT, M. N. & WHITEHOUSE, M. J. 2008. Plešovice zircon — A new natural reference material for U–Pb and Hf isotopic microanalysis. Chemical Geology, 249, 1-35.

SUN, S.-S., WARREN, R. G. & SHAW, R. D. 1995. Nd isotope study of granites from the Arunta Inlier, central Australia: constraints on geological models and limitation of the method. Precambrian Res., 71, 301-314.

SCRIMGEOUR IR, 2003. Developing a revised framework for the Arunta Region: in 'Annual Geoscience Exploration Seminar (AGES) 2003. Record of abstracts.' Northern Geological Survey, Records 2003-001

SCRIMGEOUR IR, 2013. Chapter 12: Aileron Province: in Ahmad M and Munson TJ (compilers). 'Geology and mineral resource of the Northern Territory'. Northern Territory Geological Survey, Special Publication 5.

TAYLOR, S. R. & MCCLENNAN, S. M. 1985. The Continental Crust: Its composition and Evolution, Oxford, Blackwell Scientific Publications.

VRY, J., COMPSTON, W. & CARTWRIGHT, I. 1996. SHRIMP II dating of zircons and monazites: reassessing the timing of high-grade metamorphsim and fluid flow in the Reynolds Range, northern Arunta Block, Australia. Metamorphic Geology, 14, 335-350.

WEDEPOHL, K. H. 1995. The composition of the continental crust. Geochimica et Cosmochimica Acta, 59, 1217-1232.

WORDEN KE, CARSON CJ, CLOSE DF, CONNELLAN N AND SCRIMGEOUR IR, 2008. Summary of results. Joint NTGS-GA geochronology project: Tanami Region, Arunta Region, Pine Creek Orogen and Halls Creek Orogen correlatives, January 2005 – March 2007. Northern Territory Geological Survey Record 2008-003

## APPENDIX A: LIST OF SAMPLES

| Sample # | Easting | Northing | Rock Unit | Rock Type | Geochron | Thin Section | Geochem | Isotope |
|---|---|---|---|---|---|---|---|---|
| AMJ - GP - 01a | 291157 | 7542522 | Anmatjira Orthogneiss | Megacrystic | ✓ | ✓ | ✓ | ✓ |
| AMJ - GP - 01b | 291293 | 7542580 | Anmatjira Orthogneiss | Mafic association | | ✓ | ✓ | ✓ |
| AMJ - GP - 02 | 296075 | 7535768 | Anmatjira Orthogneiss | Fine grain | | ✓ | ✓ | |
| AMJ - GP - 03 | 296075 | 7535768 | Anmatjira Orthogneiss | Megacrystic | | ✓ | ✓ | |
| AMJ - GP - 04 | 298883 | 7535540 | Aloolya Gneiss | Fine grain | | | ✓ | |
| AMJ - GP - 05 | 298883 | 7535540 | Aloolya Gneiss | Coarse grain | | ✓ | ✓ | ✓ |
| AMJ - GP - 06 | 298883 | 7535540 | Aloolya Gneiss | Mafic association | | | ✓ | |
| AMJ - GP - 07 | 298883 | 7535540 | Aloolya Gneiss | Mafic association | | ✓ | ✓ | |
| AMJ - GP - 08 | 279663 | 7549780 | Anmatjira Orthogneiss | Enriched granite | | ✓ | ✓ | |
| AMJ - GP - 09 | 279663 | 7549780 | Anmatjira Orthogneiss | Unenriched granite | | ✓ | ✓ | |
| AMJ - GP - 10 | 279663 | 7549780 | Possum Creek Charnockite | Mafic association | | ✓ | ✓ | |
| AMJ - GP - 11 | 280051 | 7550053 | Anmatjira Orthogneiss | Ingallan Creek Sand | ✓ | | | |
| AMJ - GP - 12 | 299438 | 7535524 | Aloolya Gneiss | Coarse grain | | ✓ | ✓ | |
| AMJ - GP - 13 | 318825 | 7520995 | Aloolya Gneiss | Fine grain | | | ✓ | |
| AMJ - GP -14 | 338212 | 7506466 | Aloolya Gneiss | Mafic association | | ✓ | ✓ | |
| AMJ - GP - 15 | 299686 | 7534081 | Aloolya Gneiss | Mafic association | | ✓ | ✓ | |
| AMJ - GP -16 | 299686 | 7534081 | Aloolya Gneiss | Coarse grain | | | ✓ | |
| AMJ - GP -17 | 299610 | 7533529 | Anmatjira Orthogneiss | Megacrystic | | | ✓ | |
| AMJ - GP - 18 | 299610 | 7533529 | Possum Creek Charnockite | Fine grain | | ✓ | ✓ | |
| AMJ - GP - 19 | 300015 | 7534215 | Aloolya Gneiss | Fine grain | ✓ | ✓ | ✓ | ✓ |
| AMJ - GP - 20 | 299334 | 7533952 | Possum Creek Charnockite | Ultra-Fine grain | | ✓ | ✓ | |

| | | | | | | | | |
|---|---|---|---|---|---|---|---|---|
| AMJ - GP - 21 | 300495 | 7532918 | Anmatjira Orthogneiss | Megacrystic | | ✓ | ✓ | |
| AMJ - GP - 22 | 300850 | 7532898 | Anmatjira Orthogneiss | Megacrystic | | ✓ | ✓ | |
| AMJ - GP - 23 | 302536 | 7531552 | Anmatjira Orthogneiss | Megacrystic | | ✓ | ✓ | |
| AMJ - GP - 24 | 302343 | 7531503 | Anmatjira Orthogneiss | Megacrystic | | ✓ | ✓ | ✓ |
| AMJ - GP - 25 | 301914 | 7531923 | Anmatjira Orthogneiss | Megacrystic | | ✓ | ✓ | |
| AMJ - GP - 26 | 278535 | 7542799 | Anmatjira Orthogneiss | Sand | | | | |
| AMJ - GP - 27 | 279306 | 7543793 | Anmatjira Orthogneiss | Megacrystic | | ✓ | ✓ | |
| AMJ - GP - 28 | 279282 | 7543377 | Anmatjira Orthogneiss | Sand | ✓ | | | |
| AMJ - GP - 29 | 279358 | 7542806 | Anmatjira Orthogneiss | Megacrystic | | ✓ | ✓ | |
| AMJ - GP - 30 | 288476 | 7543028 | Anmatjira Orthogneiss | Megacrystic | | ✓ | ✓ | |
| AMJ - GP - 31 | 288234 | 7547736 | Anmatjira Orthogneiss | Megacrystic | | ✓ | ✓ | |
| AMJ - GP -32 | 388372 | 7547650 | Anmatjira Orthogneiss | Megacrystic | | ✓ | ✓ | |
| AMJ - GP -33 | 289688 | 7546938 | Anmatjira Orthogneiss | Megacrystic | | ✓ | ✓ | |
| AMJ - GP - 34 | 306626 | 7523450 | Unnamed Granite | Coarse grain | | ✓ | ✓ | |
| AMJ - GP - 35 | 306742 | 7523260 | Unnamed Granite | Coarse grain | | ✓ | ✓ | |
| AMJ - GP - 36 | 306867 | 7523160 | Unnamed Granite | Coarse grain | ✓ | ✓ | ✓ | ✓ |

## APPENDIX B:GEOCHEMISTRY

**Major element geochemistry of Anmatjira Orthogneiss Samples**

| | AMJ-GP-01a | AMJ-GP-01b | AMJ-GP-02 | AMJ-GP-03 | AMJ-GP-08 | AMJ-GP-09 | AMJ-GP-17 | AMJ-GP-21 | AMJ-GP-22 |
|---|---|---|---|---|---|---|---|---|---|
| Marjor Elements (wt%) | | | | | | | | | |
| $SiO_2$ | 73.7 | 51.4 | 78.2 | 73.2 | 75.2 | 74 | 70.1 | 72.5 | 72.1 |
| $Al_2O_3$ | 13.9 | 11.15 | 12.35 | 12.5 | 12.05 | 13 | 13.45 | 13 | 12.95 |
| $Fe_2O_3$ | 2.91 | 19.45 | 1.71 | 3.02 | 2.61 | 2.74 | 3.89 | 2.83 | 3.58 |
| CaO | 1.85 | 6.73 | 0.57 | 1.43 | 1.33 | 1.1 | 1.78 | 1.59 | 1.62 |
| MgO | 0.64 | 5.32 | 0.14 | 0.58 | 0.57 | 0.51 | 0.88 | 0.58 | 0.75 |
| $Na_2O$ | 2.65 | 1.5 | 2.07 | 2.05 | 2.57 | 2.07 | 2.03 | 2.17 | 2.01 |
| $K_2O$ | 4.8 | 0.12 | 6.18 | 5.37 | 4.37 | 6.04 | 5.71 | 5.68 | 5.65 |
| $Cr_2O_3$ | <0.01 | 0.01 | <0.01 | <0.01 | <0.01 | <0.01 | <0.01 | <0.01 | <0.01 |
| $TiO_2$ | 0.43 | 2.46 | 0.11 | 0.39 | 0.4 | 0.36 | 0.58 | 0.39 | 0.48 |
| MnO | 0.03 | 0.11 | 0.04 | 0.03 | 0.01 | 0.03 | 0.04 | 0.03 | 0.03 |
| $P_2O_5$ | 0.1 | 0.28 | 0.08 | 0.11 | 0.1 | 0.09 | 0.09 | 0.08 | 0.12 |
| SrO | 0.01 | 0.01 | <0.01 | <0.01 | 0.01 | 0.01 | 0.01 | 0.01 | 0.01 |
| BaO | 0.04 | <0.01 | 0.01 | 0.04 | 0.03 | 0.04 | 0.07 | 0.05 | 0.05 |
| LOI | 0.49 | 1.14 | 0.18 | 0.25 | 0.59 | 0.66 | 0.18 | 0.25 | 0.3 |

| | AMJ-GP-23 | AMJ-GP-24 | AMJ-GP-25 | AMJ-GP-27 | AMJ-GP-29 | AMJ-GP-30 | AMJ-GP-31 | AMJ-GP-32 | AMJ-GP-33 |
|---|---|---|---|---|---|---|---|---|---|
| Marjor Elements (wt%) | | | | | | | | | |
| $SiO_2$ | 74.2 | 75.7 | 76.7 | 78.8 | 77.2 | 75.3 | 74.8 | 75.3 | 75.5 |
| $Al_2O_3$ | 11.75 | 12.25 | 12.25 | 11.4 | 12 | 11.95 | 12.35 | 12.55 | 12.35 |
| $Fe_2O_3$ | 4.19 | 2.24 | 2.54 | 1.9 | 1.22 | 2.61 | 3.05 | 2.93 | 3.53 |
| CaO | 1.34 | 1.29 | 1.4 | 0.42 | 0.56 | 1.18 | 1.58 | 1.4 | 1.5 |
| MgO | 0.83 | 0.42 | 0.47 | 0.21 | 0.18 | 0.88 | 0.65 | 0.56 | 0.63 |
| $Na_2O$ | 1.59 | 2.1 | 1.94 | 1.92 | 2.34 | 2.37 | 2.24 | 1.86 | 2 |
| $K_2O$ | 4.99 | 5.26 | 5.2 | 5.42 | 6.02 | 4.47 | 4.61 | 5.13 | 5.07 |
| $Cr_2O_3$ | <0.01 | <0.01 | <0.01 | <0.01 | <0.01 | <0.01 | <0.01 | <0.01 | <0.01 |

| | | | | | | | | | |
|---|---|---|---|---|---|---|---|---|---|
| $TiO_2$ | 0.5 | 0.32 | 0.35 | 0.18 | 0.17 | 0.41 | 0.43 | 0.4 | 0.48 |
| MnO | 0.06 | 0.02 | 0.03 | 0.02 | 0.01 | 0.03 | 0.03 | 0.05 | 0.04 |
| $P_2O_5$ | 0.11 | 0.09 | 0.11 | 0.11 | 0.15 | 0.1 | 0.1 | 0.1 | 0.11 |
| SrO | <0.01 | <0.01 | 0.01 | <0.01 | <0.01 | <0.01 | <0.01 | 0.01 | 0.01 |
| BaO | 0.05 | 0.04 | 0.04 | 0.01 | 0.02 | 0.03 | 0.04 | 0.05 | 0.04 |
| LOI | 0.67 | 0.52 | 0.34 | 0.53 | 0.7 | 0.75 | 0.64 | 0.73 | 0.55 |

Trace element geochemistry for Anmatjira Orthogneiss Samples

| | AMJ-GP-01a | AMJ-GP-01b | AMJ-GP-02 | AMJ-GP-03 | AMJ-GP-08 | AMJ-GP-09 | AMJ-GP-17 | AMJ-GP-21 | AMJ-GP-22 |
|---|---|---|---|---|---|---|---|---|---|
| Trace Elements (ppm) | | | | | | | | | |
| Ag | <0.5 | <0.5 | <0.5 | <0.5 | <0.5 | <0.5 | <0.5 | <0.5 | <0.5 |
| As | <5 | <5 | <5 | <5 | <5 | <5 | <5 | <5 | <5 |
| Ba | 357 | 6.7 | 64.6 | 354 | 312 | 391 | 631 | 451 | 413 |
| Cd | <0.5 | 1 | <0.5 | <0.5 | <0.5 | <0.5 | <0.5 | <0.5 | <0.5 |
| Co | 35 | 56 | 67 | 37 | 73 | 45 | 54 | 53 | 77 |
| Cr | 20 | 40 | 10 | 20 | 20 | 10 | 20 | 20 | 20 |
| Cs | 12.2 | 0.12 | 3.79 | 7.65 | 13.35 | 15.2 | 8.6 | 9.45 | 6.2 |
| Cu | 1 | <1 | <1 | 5 | <1 | 10 | 9 | 2 | 3 |
| Ga | 17.1 | 25.5 | 14.9 | 15.7 | 17.2 | 17 | 18.6 | 18 | 17.4 |
| Mo | <1 | <1 | <1 | <1 | <1 | <1 | <1 | <1 | <1 |
| Nb | 11.7 | 6.8 | 4.2 | 8.3 | 13.2 | 11.8 | 13.8 | 11.6 | 14.1 |
| Ni | 5 | 37 | 1 | 4 | 5 | 5 | 10 | 6 | 9 |
| Pb | 33 | 7 | 30 | 32 | 24 | 38 | 36 | 42 | 36 |
| Rb | 357 | 3.9 | 419 | 326 | 351 | 477 | 360 | 425 | 402 |
| Sc | 7 | 45 | 3 | 6 | 6 | 6 | 9 | 6 | 8 |
| Sr | 67.5 | 76.7 | 16.6 | 45.3 | 52.9 | 53.1 | 88.7 | 64.5 | 63.2 |
| Th | 47.5 | 3.78 | 12.8 | 29.3 | 56.2 | 43.6 | 55.8 | 60.3 | 37.1 |
| Tl | <10 | <10 | <10 | <10 | <10 | <10 | <10 | <10 | <10 |
| U | 11.35 | 1.15 | 1.8 | 2.98 | 17.35 | 7.85 | 4.22 | 5.61 | 4.44 |
| V | 47 | 492 | 11 | 45 | 35 | 39 | 61 | 41 | 45 |
| W | 255 | 115 | 580 | 296 | 625 | 345 | 381 | 383 | 542 |
| Y | 33.1 | 53.1 | 52.1 | 32.5 | 47.9 | 43 | 32.8 | 20.2 | 13.1 |
| Zn | 26 | 40 | 28 | 48 | 11 | 29 | 48 | 38 | 40 |
| Zr | 224 | 171 | 84 | 167 | 226 | 193 | 296 | 159 | 193 |

| | | | | | | | | | |
|---|---|---|---|---|---|---|---|---|---|
| Hf | 6.7 | 4.9 | 3 | 5.2 | 7.1 | 5.7 | 8.6 | 4.9 | 5.8 |
| Sn | 6 | 6 | 6 | 5 | 19 | 12 | 5 | 6 | 2 |
| Ta | 1.4 | 0.7 | 0.5 | 1 | 2.4 | 1.7 | 1.5 | 1.1 | 1.3 |
| Li | 10 | 10 | 20 | 20 | 40 | 20 | 20 | 20 | 20 |

| | AMJ-GP-23 | AMJ-GP-24 | AMJ-GP-25 | AMJ-GP-27 | AMJ-GP-29 | AMJ-GP-30 | AMJ-GP-31 | AMJ-GP-32 | AMJ-GP-33 |
|---|---|---|---|---|---|---|---|---|---|
| Trace Elements (ppm) | | | | | | | | | |
| Ag | <0.5 | <0.5 | <0.5 | <0.5 | <0.5 | <0.5 | <0.5 | <0.5 | <0.5 |
| As | <5 | <5 | <5 | <5 | <5 | <5 | <5 | <5 | <5 |
| Ba | 417 | 345 | 353 | 103.5 | 154 | 249 | 305 | 418 | 366 |
| Cd | <0.5 | <0.5 | <0.5 | <0.5 | <0.5 | <0.5 | <0.5 | <0.5 | <0.5 |
| Co | 70 | 56 | 53 | 73 | 76 | 61 | 59 | 69 | 68 |
| Cr | 20 | 10 | 10 | 10 | 10 | 20 | 20 | 10 | 10 |
| Cs | 13.55 | 6.38 | 7.07 | 28.5 | 10.8 | 12.55 | 12.3 | 4.48 | 20.9 |
| Cu | 8 | 4 | 2 | <1 | <1 | 2 | 6 | 2 | 14 |
| Ga | 16.8 | 16.4 | 16.8 | 15.9 | 16.2 | 17.6 | 17 | 16.6 | 18.2 |
| Mo | <1 | <1 | <1 | <1 | <1 | <1 | <1 | <1 | <1 |
| Nb | 12.3 | 9.9 | 10.8 | 12.4 | 12 | 11.8 | 12.3 | 10.7 | 13 |
| Ni | 8 | 5 | 4 | 2 | 2 | 6 | 7 | 3 | 6 |
| Pb | 35 | 35 | 32 | 23 | 24 | 28 | 30 | 35 | 36 |
| Rb | 378 | 396 | 431 | 654 | 630 | 365 | 378 | 326 | 427 |
| Sc | 10 | 4 | 4 | 4 | 3 | 6 | 7 | 6 | 7 |
| Sr | 59.9 | 50.2 | 59.5 | 23.7 | 31.7 | 62.3 | 57.2 | 58.7 | 63.2 |
| Th | 38.5 | 34.1 | 48.8 | 38.3 | 34.9 | 46.7 | 43.2 | 41.3 | 48.5 |
| Tl | <10 | <10 | <10 | <10 | <10 | <10 | <10 | <10 | <10 |
| U | 3.75 | 4.09 | 4.4 | 11.95 | 23.7 | 6.12 | 6.6 | 7.61 | 10.75 |
| V | 53 | 37 | 35 | 18 | 16 | 41 | 40 | 42 | 38 |
| W | 489 | 428 | 471 | 639 | 650 | 505 | 442 | 508 | 527 |
| Y | 53 | 26.9 | 26.3 | 59.3 | 55.7 | 51.9 | 48.3 | 37.1 | 37.7 |
| Zn | 47 | 24 | 23 | 10 | 6 | 29 | 34 | 34 | 41 |
| Zr | 199 | 140 | 227 | 113 | 102 | 194 | 202 | 206 | 231 |
| Hf | 5.7 | 4.4 | 6.8 | 4.3 | 3.6 | 5.9 | 6.1 | 6.1 | 7.1 |

| | | | | | | | | | |
|---|---|---|---|---|---|---|---|---|---|
| Sn | 8 | 7 | 4 | 21 | 14 | 15 | 12 | 11 | 14 |
| Ta | 1.5 | 1.1 | 1.1 | 2.4 | 2.5 | 1.6 | 1.6 | 1.3 | 1.8 |
| Li | 30 | 20 | 20 | 40 | 10 | 10 | 10 | 10 | 30 |

**Rare Earth Elements Geochemistry for the Anmatjira Orthogneiss**

| | AMJ-GP-01a | AMJ-GP-01b | AMJ-GP-02 | AMJ-GP-03 | AMJ-GP-08 | AMJ-GP-09 | AMJ-GP-17 | AMJ-GP-21 | AMJ-GP-22 |
|---|---|---|---|---|---|---|---|---|---|
| REE (ppm) | | | | | | | | | |
| La | 49.5 | 21.6 | 17.6 | 45.7 | 53.3 | 62.3 | 76.1 | 70.2 | 59.8 |
| Ce | 102.5 | 46.7 | 37.1 | 89.7 | 119.5 | 115 | 149 | 141.5 | 119.5 |
| Pr | 10.25 | 5.59 | 3.86 | 9.85 | 11.7 | 11.7 | 15.25 | 14.1 | 12 |
| Nd | 34.8 | 24.4 | 12.4 | 33.7 | 38.9 | 38.4 | 52.5 | 48.1 | 39 |
| Sm | 7.34 | 6.79 | 2.94 | 6.72 | 8.08 | 7.8 | 9.97 | 9.31 | 6.82 |
| Eu | 0.82 | 2.83 | 0.24 | 0.79 | 0.75 | 0.75 | 1.22 | 0.88 | 0.87 |
| Gd | 6.29 | 8.61 | 3.88 | 6.16 | 7.59 | 7.11 | 8.33 | 7.59 | 5.08 |
| Tb | 1.05 | 1.51 | 0.94 | 0.93 | 1.27 | 1.17 | 1.2 | 0.98 | 0.71 |
| Dy | 5.72 | 9.18 | 7.15 | 5.43 | 7.22 | 6.76 | 5.95 | 4.47 | 2.79 |
| Ho | 1.08 | 1.96 | 1.78 | 1.21 | 1.67 | 1.37 | 1.19 | 0.72 | 0.44 |
| Er | 3.13 | 5.87 | 5.46 | 3.33 | 4.84 | 3.87 | 3.07 | 1.44 | 1.02 |
| Tm | 0.4 | 0.82 | 0.78 | 0.46 | 0.66 | 0.56 | 0.42 | 0.15 | 0.14 |
| Yb | 2.51 | 5.14 | 4.76 | 2.91 | 4.32 | 3.53 | 2.63 | 0.89 | 0.73 |
| Lu | 0.35 | 0.81 | 0.61 | 0.44 | 0.63 | 0.51 | 0.43 | 0.15 | 0.13 |

| | AMJ-GP-23 | AMJ-GP-24 | AMJ-GP-25 | AMJ-GP-27 | AMJ-GP-29 | AMJ-GP-30 | AMJ-GP-31 | AMJ-GP-32 | AMJ-GP-33 |
|---|---|---|---|---|---|---|---|---|---|
| REE (ppm) | | | | | | | | | |
| La | 49.1 | 49.3 | 39 | 29.3 | 23.1 | 52.8 | 55.3 | 25.6 | 40.9 |
| Ce | 97.1 | 96.8 | 112 | 63.1 | 53.2 | 114 | 111.5 | 99.4 | 106 |
| Pr | 10.25 | 10.35 | 8.77 | 6.7 | 5.33 | 10.9 | 11.25 | 5.49 | 9.35 |
| Nd | 35.7 | 36.7 | 29.3 | 22.3 | 18.2 | 37.4 | 38.7 | 19.2 | 30.6 |
| Sm | 7.54 | 8.04 | 6.57 | 6.15 | 5.2 | 7.98 | 8.55 | 4.48 | 6.92 |
| Eu | 0.87 | 0.76 | 0.7 | 0.26 | 0.31 | 0.69 | 0.83 | 0.5 | 0.69 |

| | | | | | | | | | |
|---|---|---|---|---|---|---|---|---|---|
| Gd | 7.52 | 7.11 | 5.78 | 6.61 | 6.06 | 7.35 | 7.76 | 4.78 | 5.94 |
| Tb | 1.41 | 1.12 | 0.98 | 1.46 | 1.29 | 1.39 | 1.37 | 0.92 | 1.13 |
| Dy | 8.16 | 5.54 | 4.85 | 9.02 | 8.14 | 7.89 | 7.44 | 5.82 | 6.19 |
| Ho | 1.76 | 0.93 | 0.94 | 1.9 | 1.79 | 1.72 | 1.54 | 1.25 | 1.3 |
| Er | 4.92 | 2.01 | 2.5 | 5.85 | 5.27 | 4.83 | 4.62 | 3.44 | 3.55 |
| Tm | 0.73 | 0.25 | 0.31 | 0.88 | 0.77 | 0.67 | 0.68 | 0.5 | 0.5 |
| Yb | 4.59 | 1.12 | 2 | 5.5 | 5.08 | 4.35 | 3.99 | 2.98 | 3.01 |
| Lu | 0.66 | 0.15 | 0.31 | 0.71 | 0.71 | 0.65 | 0.59 | 0.45 | 0.47 |

**Major element geochemistry of Aloolya Gneiss Samples**

| | AMJ-GP-04 | AMJ-GP-05 | AMJ-GP-06 | AMJ-GP-07 | AMJ-GP-12 | AMJ-GP-13 | AMJ-GP-14 | AMJ-GP-15 | AMJ-GP-16 | AMJ-GP-19 |
|---|---|---|---|---|---|---|---|---|---|---|
| Marjor Elements (wt%) | | | | | | | | | | |
| $SiO_2$ | 78.5 | 76.6 | 54.5 | 55.4 | 79.5 | 80.4 | 55.2 | 49.4 | 78.1 | 78.1 |
| $Al_2O_3$ | 11.75 | 12.55 | 15.9 | 15.25 | 11.2 | 10.7 | 14.45 | 11.1 | 11.55 | 11.55 |
| $Fe_2O_3$ | 0.57 | 1.17 | 10.55 | 11.5 | 1.48 | 0.48 | 12.25 | 20 | 2.12 | 0.24 |
| CaO | 0.47 | 0.95 | 9.86 | 9.94 | 0.76 | 0.43 | 9.19 | 7.74 | 0.92 | 0.49 |
| MgO | 0.13 | 0.29 | 5.87 | 5.91 | 0.29 | 0.09 | 5.43 | 3.64 | 0.41 | 0.04 |
| $Na_2O$ | 1.74 | 1.85 | 1.02 | 1.18 | 1.9 | 1.7 | 2.12 | 0.7 | 1.76 | 1.76 |
| $K_2O$ | 6.96 | 6.73 | 1.03 | 0.96 | 5.23 | 5.92 | 1.45 | 1.47 | 5.97 | 6.76 |
| $Cr_2O_3$ | <0.01 | <0.01 | 0.02 | 0.02 | <0.01 | <0.01 | 0.02 | <0.01 | <0.01 | <0.01 |
| $TiO_2$ | 0.11 | 0.18 | 0.77 | 0.91 | 0.16 | 0.07 | 1.11 | 2.66 | 0.36 | 0.04 |
| MnO | 0.01 | 0.01 | 0.16 | 0.16 | 0.02 | <0.01 | 0.17 | 0.28 | 0.01 | <0.01 |
| $P_2O_5$ | 0.05 | 0.07 | 0.12 | 0.11 | 0.08 | 0.06 | 0.16 | 0.28 | 0.06 | 0.11 |
| SrO | 0.01 | <0.01 | 0.01 | 0.01 | <0.01 | <0.01 | 0.01 | <0.01 | <0.01 | <0.01 |
| BaO | 0.03 | 0.04 | 0.02 | 0.03 | 0.02 | 0.03 | 0.04 | 0.07 | 0.03 | 0.01 |
| LOI | 0.21 | 0.22 | 0.08 | 0.01 | 0.31 | 0.35 | -0.11 | 0.69 | 0.28 | 0.24 |

**Trace element geochemistry for Aloolya Gneiss Samples**

| | AMJ-GP-04 | AMJ-GP-05 | AMJ-GP-06 | AMJ-GP-07 | AMJ-GP-12 | AMJ-GP-13 | AMJ-GP-14 | AMJ-GP-15 | AMJ-GP-16 | AMJ-GP-19 |
|---|---|---|---|---|---|---|---|---|---|---|
| Trace Elements (ppm) | | | | | | | | | | |
| Ag | <0.5 | <0.5 | <0.5 | <0.5 | <0.5 | <0.5 | <0.5 | <0.5 | <0.5 | <0.5 |
| As | <5 | <5 | <5 | <5 | <5 | <5 | <5 | <5 | <5 | <5 |
| Ba | 282 | 325 | 211 | 241 | 173.5 | 237 | 328 | 616 | 239 | 90.3 |
| Cd | <0.5 | <0.5 | <0.5 | 0.5 | <0.5 | <0.5 | 0.5 | 0.9 | <0.5 | <0.5 |
| Co | 66 | 60 | 70 | 66 | 41 | 70 | 68 | 78 | 62 | 36 |
| Cr | 10 | 10 | 200 | 140 | 10 | 10 | 130 | 20 | 10 | <10 |
| Cs | 3.75 | 4.07 | 6.5 | 3.38 | 6.86 | 3.63 | 1.32 | 3 | 8.01 | 4.06 |
| Cu | <1 | <1 | 62 | 82 | <1 | <1 | 49 | 135 | 2 | <1 |
| Ga | 11.1 | 13.3 | 18.2 | 17.1 | 13.9 | 13.5 | 19.9 | 23.7 | 16.9 | 11.5 |
| Mo | <1 | <1 | <1 | <1 | <1 | <1 | <1 | <1 | <1 | <1 |
| Nb | 2.3 | 4.1 | 5.7 | 6.4 | 5.7 | 1.9 | 8.9 | 7.3 | 11.1 | 1.5 |
| Ni | 2 | 3 | 106 | 102 | 2 | 1 | 68 | 29 | 6 | 1 |
| Pb | 54 | 44 | 8 | 9 | 26 | 29 | 12 | 7 | 40 | 45 |
| Rb | 354 | 342 | 115.5 | 71.5 | 365 | 423 | 64.4 | 87.6 | 400 | 472 |
| Sc | 1 | 2 | 30 | 34 | 2 | 1 | 34 | 45 | 4 | <1 |
| Sr | 47.7 | 44.9 | 80.6 | 84.9 | 46.2 | 35.3 | 83.6 | 37.8 | 37.1 | 24.9 |
| Th | 14.05 | 31.8 | 4 | 4.44 | 15.05 | 11 | 2.09 | 3.18 | 48.6 | 19.85 |
| Tl | <10 | <10 | <10 | <10 | <10 | <10 | <10 | <10 | <10 | <10 |
| U | 1.16 | 3.14 | 0.96 | 0.91 | 3.54 | 1.25 | 0.38 | 1.2 | 5.3 | 2.87 |
| V | 18 | 14 | 220 | 232 | 23 | 18 | 265 | 464 | 35 | 7 |
| W | 574 | 518 | 267 | 180 | 331 | 589 | 192 | 176 | 501 | 317 |
| Y | 4.4 | 20.2 | 27.3 | 30.3 | 30.5 | 14.9 | 37.7 | 60.6 | 28.2 | 31.2 |
| Zn | 8 | 20 | 92 | 95 | 19 | 17 | 106 | 149 | 33 | 6 |
| Zr | 24 | 144 | 142 | 146 | 139 | 43 | 183 | 180 | 209 | 79 |

| | | | | | | | | | | |
|---|---|---|---|---|---|---|---|---|---|---|
| Hf | 0.8 | 4.3 | 4 | 3.8 | 4.5 | 1.4 | 4.9 | 5.2 | 6.4 | 2.9 |
| Sn | 4 | 4 | 8 | 4 | 5 | 7 | 4 | 15 | 7 | 3 |
| Ta | 0.3 | 0.6 | 0.7 | 0.7 | 0.9 | 0.3 | 0.8 | 0.7 | 1.1 | 0.3 |
| Li | 30 | 20 | 10 | 10 | 30 | <10 | 20 | <10 | 20 | <10 |

**Rare Earth Elements Geochemistry for the Aloolya Gneiss**

| REE (ppm) | AMJ-GP-04 | AMJ-GP-05 | AMJ-GP-06 | AMJ-GP-07 | AMJ-GP-12 | AMJ-GP-13 | AMJ-GP-14 | AMJ-GP-15 | AMJ-GP-16 | AMJ-GP-19 |
|---|---|---|---|---|---|---|---|---|---|---|
| La | 18 | 46 | 22.2 | 22.6 | 21.8 | 17.1 | 28.2 | 19.8 | 52.2 | 18.1 |
| Ce | 29.9 | 91.7 | 42.3 | 45 | 41.2 | 33.1 | 56.9 | 43.5 | 105.5 | 35.2 |
| Pr | 3.01 | 9.59 | 4.82 | 5.27 | 4.28 | 3.27 | 6.05 | 5.23 | 10.95 | 3.49 |
| Nd | 10 | 33 | 18.6 | 20.3 | 14.1 | 11 | 24 | 22.6 | 36.5 | 12 |
| Sm | 1.96 | 7.05 | 3.9 | 4.7 | 3.42 | 2.42 | 5.85 | 6.8 | 7.62 | 3.16 |
| Eu | 0.71 | 0.63 | 1.16 | 1.22 | 0.47 | 0.45 | 1.26 | 2.04 | 0.6 | 0.39 |
| Gd | 1.66 | 6.15 | 4.66 | 5.12 | 3.29 | 2.31 | 6.08 | 8.72 | 7.03 | 3.73 |
| Tb | 0.21 | 0.82 | 0.73 | 0.8 | 0.69 | 0.47 | 1.01 | 1.61 | 1.07 | 0.8 |
| Dy | 1.05 | 3.89 | 4.53 | 5.09 | 4.33 | 2.39 | 5.95 | 9.3 | 5.16 | 4.63 |
| Ho | 0.14 | 0.71 | 1 | 1.09 | 1.03 | 0.51 | 1.35 | 1.99 | 0.96 | 1 |
| Er | 0.38 | 1.8 | 3.01 | 3.45 | 3.17 | 1.17 | 3.77 | 5.98 | 2.29 | 2.62 |
| Tm | 0.04 | 0.24 | 0.44 | 0.48 | 0.51 | 0.15 | 0.53 | 0.9 | 0.32 | 0.32 |
| Yb | 0.23 | 1.44 | 2.88 | 3.17 | 3.36 | 0.71 | 3.68 | 5.46 | 1.62 | 1.82 |
| Lu | 0.06 | 0.21 | 0.44 | 0.46 | 0.51 | 0.1 | 0.55 | 0.85 | 0.25 | 0.23 |

**Major element geochemistry of the Un-named Granite**

| | AMJ-GP-34 | AMJ-GP-35 | AMJ-GP-36 |
|---|---|---|---|
| Marjor Elements (wt%) | | | |
| $SiO_2$ | 72.9 | 71.9 | 72.9 |
| $Al_2O_3$ | 12.65 | 14.05 | 13.9 |
| $Fe_2O_3$ | 4.84 | 3.82 | 3.34 |
| CaO | 2.04 | 2.01 | 1.81 |
| MgO | 1.08 | 0.94 | 0.84 |
| $Na_2O$ | 1.65 | 1.92 | 1.89 |
| K2O | 3.67 | 5.22 | 5.63 |
| $Cr_2O_3$ | <0.01 | <0.01 | <0.01 |
| $TiO_2$ | 0.49 | 0.51 | 0.41 |
| MnO | 0.07 | 0.05 | 0.04 |
| $P_2O_5$ | 0.06 | 0.09 | 0.1 |
| SrO | 0.01 | 0.01 | 0.01 |
| BaO | 0.07 | 0.1 | 0.11 |
| LOI | -0.05 | 0.08 | 0.14 |

**Trace element geochemistry for the Un-named Granite**

| | AMJ-GP-34 | AMJ-GP-35 | AMJ-GP-36 |
|---|---|---|---|
| Trace Elements (ppm) | | | |
| Ag | <0.5 | <0.5 | <0.5 |
| As | <5 | <5 | <5 |
| Ba | 660 | 915 | 993 |
| Cd | <0.5 | <0.5 | <0.5 |
| Co | 88 | 69 | 51 |
| Cr | 30 | 30 | 20 |
| Cs | 0.88 | 1.72 | 1.4 |
| Cu | 11 | 13 | 7 |
| Ga | 17 | 19.8 | 18.1 |
| Mo | <1 | <1 | <1 |
| Nb | 10.4 | 10.7 | 8.4 |
| Ni | 11 | 11 | 9 |
| Pb | 27 | 33 | 40 |
| Rb | 167.5 | 258 | 263 |
| Sc | 13 | 9 | 7 |
| Sr | 105.5 | 128 | 132 |
| Th | 54.8 | 49.8 | 29.9 |
| Tl | <10 | <10 | <10 |
| U | 2.47 | 2.75 | 1.34 |
| V | 55 | 54 | 45 |
| W | 689 | 543 | 397 |
| Y | 69.4 | 44.9 | 39.6 |
| Zn | 67 | 43 | 35 |
| Zr | 266 | | |
| Hf | 7.6 | 7.7 | 5.6 |
| Sn | 2 | 4 | 3 |
| Ta | 1 | 0.9 | 0.7 |
| Li | 20 | 10 | 10 |

**Rare Earth Elements Geochemistry for the Un-named Granite**

| | AMJ-GP-34 | AMJ-GP-35 | AMJ-GP-36 |
|---|---|---|---|
| REE (ppm) | | | |
| La | 88.3 | 86.1 | 57.9 |
| Ce | 178.5 | | |
| Pr | 17.9 | 17.85 | 11.45 |
| Nd | 63.6 | 63 | 40.5 |
| Sm | 12.75 | 12.6 | 7.98 |
| Eu | 1.23 | 1.55 | 1.54 |
| Gd | 12.2 | 10.45 | 7.8 |
| Tb | 1.9 | 1.54 | 1.2 |
| Dy | 11.1 | 7.96 | 6.47 |
| Ho | 2.35 | 1.6 | 1.34 |
| Er | 7.07 | 3.91 | 3.54 |
| Tm | 1.04 | 0.56 | 0.51 |
| Yb | 7.25 | 3.16 | 3.23 |
| Lu | 1.11 | 0.49 | 0.5 |

**Major element geochemistry of the Possum Creek Charnockite**

| | AMJ-GP-10 | AMJ-GP-18 | AMJ-GP-20 |
|---|---|---|---|
| Marjor Elements (wt%) | | | |
| $SiO_2$ | 73.2 | 69.3 | 73.3 |
| $Al_2O_3$ | 13.1 | 12.65 | 12 |
| $Fe_2O_3$ | 3.19 | 5.26 | 3.11 |
| CaO | 1.2 | 2.4 | 1.43 |
| MgO | 0.68 | 0.8 | 0.47 |
| $Na_2O$ | 2.34 | 2.01 | 1.72 |
| K2O | 5.53 | 5.54 | 5.16 |
| $Cr_2O_3$ | <0.01 | <0.01 | <0.01 |
| $TiO_2$ | 0.43 | 0.6 | 0.61 |
| MnO | 0.02 | 0.07 | 0.04 |
| $P_2O_5$ | 0.11 | 0.19 | 0.1 |
| SrO | 0.01 | 0.01 | <0.01 |
| BaO | 0.05 | 0.06 | 0.06 |
| LOI | 0.54 | 0.08 | 0.28 |

**Trace element geochemistry for the Possum Creek Charnockite**

| | AMJ-GP-10 | AMJ-GP-18 | AMJ-GP-20 |
|---|---|---|---|
| Trace Elements (ppm) | | | |
| Ag | <0.5 | <0.5 | <0.5 |
| As | <5 | <5 | <5 |
| Ba | 426 | 547 | 476 |
| Cd | <0.5 | <0.5 | <0.5 |
| Co | 50 | 57 | 60 |
| Cr | 20 | 10 | 10 |
| Cs | 31.2 | 2.43 | 5.7 |
| Cu | 9 | 13 | 3 |

| | | | |
|---|---|---|---|
| Ga | 16.4 | 18.8 | 15.2 |
| Mo | <1 | <1 | <1 |
| Nb | 11.5 | 15.3 | 14 |
| Ni | 6 | 4 | 5 |
| Pb | 27 | 25 | 40 |
| Rb | 516 | 332 | 300 |
| Sc | 7 | 25 | 7 |
| Sr | 58.1 | 64.4 | 45.6 |
| Th | 45.1 | 22.1 | 64.4 |
| Tl | <10 | <10 | <10 |
| U | 7.48 | 1.13 | 3.21 |
| V | 46 | 70 | 47 |
| W | 354 | 399 | 442 |
| Y | 38.5 | 76.3 | 35.3 |
| Zn | 15 | 59 | 35 |
| Zr | 205 | 291 | 450 |
| Hf | 6.2 | 8 | 12 |
| Sn | 14 | 3 | 3 |
| Ta | 1.6 | 1.2 | 1.4 |
| Li | 90 | 10 | 20 |

**Rare Earth Elements Geochemistry for the Possum Creek Charnockite**

| | AMJ-GP-10 | AMJ-GP-18 | AMJ-GP-20 |
|---|---|---|---|
| REE (ppm) | | | |
| La | 42.4 | 64.9 | 88.3 |
| Ce | 89.7 | 131.5 | 178.5 |
| Pr | 8.96 | 14.7 | 17 |
| Nd | 30.1 | 55.7 | 58.6 |
| Sm | 6.34 | 14.15 | 9.85 |
| Eu | 0.62 | 1.42 | 0.97 |
| Gd | 6.27 | 14.8 | 8.29 |
| Tb | 1.11 | 2.62 | 1.19 |
| Dy | 6.26 | 14.25 | 6.18 |
| Ho | 1.34 | 2.9 | 1.19 |
| Er | 3.71 | 7.28 | 3.43 |
| Tm | 0.55 | 0.88 | 0.45 |
| Yb | 3.31 | 4.75 | 2.7 |
| Lu | 0.5 | 0.64 | 0.39 |

## APPENDIX C: GEOCHRONOLOGY

| Analyses # | U | Th | 207Pb/206Pb Age (Ma) | Pb206/U238 | Pb207/U235 | Discordance (%) |
|---|---|---|---|---|---|---|
| **Anmatjira Orthogneiss** | | | | | | |
| Igneous Crystallisation | | | | | | |
| 01A-02 | 826549 | 222624 | 1779.4 | 1754.3 | 1765.8 | -1 |
| 01A-05 | 601333 | 109933 | 1774.7 | 1764 | 1768.9 | -1 |
| 01A-07 | 502438 | 304149 | 1755.3 | 1598.9 | 1667.6 | -9 |
| 01A-08 | 1362435 | 312184 | 1756.7 | 1705.1 | 1728.4 | -3 |
| 01A-09 | 1199957 | 234191 | 1779.3 | 1647.9 | 1706.5 | -7 |
| 01A-11 | 655887 | 298222 | 1802.7 | 1630.4 | 1707.1 | -10 |
| 01A-34 | 958325 | 224938 | 1771.9 | 1691.3 | 1727.5 | -5 |
| 01A-40 | 3654068 | 237712 | 1791.5 | 1603.6 | 1686.5 | -10 |
| 01A-43 | 1185197 | 509552 | 1792.9 | 1641.6 | 1709.3 | -8 |
| 01A-44 | 1650144 | 213626 | 1770.7 | 1761.5 | 1765.7 | -1 |
| 01A-45 | 1234383 | 272340 | 1784.9 | 1708.1 | 1742.9 | -4 |
| 01A-47 | 828102 | 708839 | 1794.8 | 1758.9 | 1775.5 | -2 |
| 01A-49 | 463226 | 215431 | 1800.6 | 1641.4 | 1712.5 | -9 |
| 01A-63 | 985897 | 210939 | 1793.3 | 1799 | 1796.3 | 0 |
| 01A-66 | 862256 | 204287 | 1758.9 | 1617.2 | 1679.6 | -8 |
| 01A-67 | 685320 | 148954 | 1758.4 | 1778 | 1768.8 | 1 |
| 01A-72 | 931574 | 57152 | 1786.9 | 1664.5 | 1719.2 | -7 |
| 01A78 | 754403 | 91443 | 1798.6 | 1704.8 | 1747.5 | -5 |
| 01A84 | 1100846 | 245820 | 1801 | 1674.9 | 1731.6 | -7 |
| 01A85 | 663939 | 320073 | 1797.2 | 1671.3 | 1727.9 | -7 |
| 01A86 | 402521 | 91878 | 1803.3 | 1639.9 | 1712.8 | -9 |
| 01A92 | 475284 | 96569 | 1776.1 | 1726.1 | 1748.8 | -3 |
| 01A95 | 233666 | 29888 | 1769.5 | 1776.6 | 1773.3 | 0 |
| 01A99 | 432521 | 136198 | 1781.3 | 1615.1 | 1688.6 | -9 |
| 01A103 | 527978 | 68571 | 1776.9 | 1718.5 | 1744.9 | -3 |
| 01A104 | 601156 | 153202 | 1774.2 | 1749.2 | 1760.5 | -1 |
| 01A110 | 302032 | 183420 | 1801.5 | 1669.1 | 1728.8 | -7 |
| 01A117 | 515135 | 57799 | 1769.1 | 1830 | 1801.7 | 3 |
| 01A126 | 363054 | 79440 | 1756.1 | 1707 | 1729.1 | -3 |

| | | | | | | |
|---|---|---|---|---|---|---|
| 01A128 | 280756 | 60999 | 1789.1 | 1750.5 | 1768 | -2 |
| 01A130 | 333038 | 38376 | 1781.5 | 1730.8 | 1753.7 | -3 |
| 01A131 | 524350 | 134382 | 1790 | 1717 | 1750.1 | -4 |
| 01A138 | 957689 | 133432 | 1803.9 | 1682.5 | 1737.5 | -7 |
| 01A141 | 680987 | 142511 | 1809.4 | 1691.9 | 1745.1 | -6 |
| 01A142 | 178653 | 21761 | 1800.3 | 1740.8 | 1768.1 | -3 |
| 01A144 | 1008720 | 103207 | 1784.8 | 1713 | 1745.6 | -4 |
| 01A145 | 703193 | 214417 | 1805.8 | 1717.5 | 1757.6 | -5 |
| 01A147 | 617171 | 66825 | 1790.5 | 1727.9 | 1756.4 | -3 |
| 01A149 | 261046 | 59852 | 1808.5 | 1777.4 | 1791.7 | -2 |
| 01A150 | 348985 | 58389 | 1801.1 | 1723 | 1758.6 | -4 |
| 01A152 | 297759 | 117539 | 1797.4 | 1664.6 | 1724.1 | -7 |
| 01A156 | 331316 | 49797 | 1766.1 | 1746.6 | 1755.7 | -1 |
| 01A157 | 824304 | 193580 | 1803.7 | 1700.8 | 1747.6 | -6 |
| 01A158 | 184321 | 24719 | 1792.2 | 1760.6 | 1775.2 | -2 |
| 01A159 | 475544 | 79665 | 1795.6 | 1719.7 | 1754.2 | -4 |
| 01A160 | 323400 | 65950 | 1780.3 | 1715.3 | 1744.8 | -4 |
| 01A162 | 325528 | 54160 | 1770.9 | 1765.6 | 1768.1 | 0 |
| 01A163 | 648631 | 104358 | 1795 | 1785.5 | 1789.8 | -1 |
| 01A185 | 702487 | 92708 | 1792.4 | 1807.8 | 1800.6 | 1 |
| 11A02 | 278918 | 47459 | 1751 | 1768.2 | 1760.3 | 1 |
| 11A07 | 362853 | 172410 | 1803.3 | 1676.4 | 1733.5 | -7 |
| 11A012 | 386256 | 68694 | 1798.1 | 1776.9 | 1786.6 | -1 |
| 11A24 | 562061 | 54302 | 1777.7 | 1759.7 | 1768.2 | -1 |
| 11A25 | 274248 | 82874 | 1801.6 | 1796.9 | 1799.3 | 0 |
| 11A26 | 298889 | 143195 | 1782.7 | 1652.6 | 1711 | -7 |
| 11A27 | 402548 | 71442 | 1760.5 | 1799.2 | 1781.5 | 2 |
| 11A29 | 507442 | 88852 | 1773.9 | 1770.8 | 1772.3 | 0 |
| 11A30 | 622977 | 91744 | 1751.5 | 1830.7 | 1794 | 5 |
| 11A39 | 880198 | 204848 | 1801.6 | 1659 | 1722.9 | -8 |
| 11A40 | 1437398 | 885791 | 1775.6 | 1715.9 | 1742.8 | -3 |
| 11A41 | 1786176 | 562777 | 1790.7 | 1793.2 | 1791.9 | 0 |
| 11A45 | 1422057 | 210495 | 1798.9 | 1848.3 | 1825.1 | 3 |
| 11A48 | 1245123 | 165351 | 1782.2 | 1893.4 | 1840.9 | 6 |
| 28A07 | 1209735 | 862548 | 1787.9 | 1644 | 1708.2 | -8 |
| 28A24 | 465559 | 107514 | 1813.1 | 1737.5 | 1772.3 | -4 |
| 28A30 | 1160272 | 212775 | 1815.6 | 1734.2 | 1771.5 | -4 |
| 28A44 | 1145904 | 188666 | 1796.7 | 1795.9 | 1796.1 | 0 |
| 28A45 | 570608 | 211303 | 1800.8 | 1674.6 | 1731.4 | -7 |
| 28A47 | 619511 | 55808 | 1791.7 | 1749.6 | 1768.8 | -2 |
| 28A61 | 1258068 | 387987 | 1782.3 | 1725.5 | 1751.2 | -3 |
| 28A70 | 756707 | 149431 | 1810.7 | 1744.5 | 1774.7 | -4 |
| 28A74 | 929373 | 207132 | 1792.8 | 1621.5 | 1697.5 | -10 |
| 28A80 | 804047 | 52427 | 1804.2 | 1642 | 1714.4 | -9 |

| | | | | | | |
|---|---|---|---|---|---|---|
| 28A82 | 501351 | 90180 | 1804.1 | 1654.2 | 1721.1 | -8 |
| 28A83 | 754603 | 141554 | 1788.4 | 1615 | 1691.8 | -10 |
| 28A96 | 825855 | 220960 | 1808.7 | 1718.8 | 1759.5 | -5 |
| 28A103 | 790657 | 260244 | 1800.2 | 1765 | 1781.1 | -2 |
| 28A116 | 192965 | 103097 | 1786.8 | 1691.3 | 1734.1 | -5 |
| 28A122 | 2470807 | 2064223 | 1790.3 | 1902.7 | 1849.5 | 6 |
| 28A137 | 631735 | 142239 | 1789.5 | 1784.6 | 1786.7 | 0 |
| 28A142 | 946779 | 279734 | 1796.9 | 1673 | 1728.6 | -7 |
| Inherited Zircons | | | | | | |
| 01A-03 | 1168415 | 297609 | 1876.8 | 1502.6 | 1665.1 | -20 |
| 01A-04 | 4187474 | 2441588 | 1919.1 | 932.1 | 1278.1 | -51 |
| 01A-07 | 502438 | 304149 | 1755.3 | 1598.9 | 1667.6 | -9 |
| 01A-08 | 1362435 | 312184 | 1756.7 | 1705.1 | 1728.4 | -3 |
| 01A-09 | 1199957 | 234191 | 1779.3 | 1647.9 | 1706.5 | -7 |
| 01A-10 | 1000800 | 136558 | 1724.1 | 1687.4 | 1703.8 | -2 |
| 01A-11 | 655887 | 298222 | 1802.7 | 1630.4 | 1707.1 | -10 |
| 01A-12 | 1950707 | 1686361 | 1846.8 | 1400.4 | 1587.9 | -24 |
| 01A-14 | 896110 | 435611 | 1891.2 | 1284.6 | 1531.4 | -32 |
| 01A-18 | 1467851 | 555429 | 1810.6 | 1251.9 | 1474.2 | -31 |
| 01A-19 | 1326203 | 355489 | 1902.3 | 1581.8 | 1724.5 | -17 |
| 01A-23 | 2164298 | 1248967 | 1919.6 | 1251.1 | 1520.8 | -35 |
| 01A-24 | 1994876 | 619052 | 1962.7 | 1216.3 | 1515.4 | -38 |
| 01A-25 | 1260178 | 2645878 | 1850.3 | 774.9 | 1112.9 | -58 |
| 01A-26 | 1368542 | 471423 | 1822.3 | 1522.5 | 1652.5 | -16 |
| 01A-28 | 664346 | 348216 | 1814.4 | 1210.2 | 1446.9 | -33 |
| 01A-29 | 1669292 | 516048 | 1966 | 951.8 | 1313.7 | -52 |
| 01A-31 | 942481 | 840117 | 1808.5 | 1521.8 | 1646 | -16 |
| 01A-38 | 621880 | 223390 | 1843.8 | 1662.4 | 1744.1 | -10 |
| 01A-46 | 1578941 | 254823 | 2030.8 | 1369.1 | 1650.9 | -33 |
| 01A-48 | 818294 | 245744 | 1844 | 1662.3 | 1744.2 | -10 |
| 01A-49 | 463226 | 215431 | 1800.6 | 1641.4 | 1712.5 | -9 |
| 01A-51 | 2568967 | 1204628 | 1898.2 | 910 | 1251.2 | -52 |
| 01A-53 | 1000769 | 191790 | 1866.1 | 1584.5 | 1709.5 | -15 |
| 01A-56 | 1821137 | 1538827 | 1850.9 | 1382.2 | 1578.2 | -25 |
| 01A-58 | 636172 | 342458 | 1893.4 | 1591 | 1725.8 | -16 |
| 01A-59 | 2221056 | 1496008 | 1806 | 1095.8 | 1360.8 | -39 |
| 01A-61 | 1253379 | 812220 | 1935.7 | 1535.5 | 1712.1 | -21 |
| 01A-62 | 688246 | 275708 | 1820.1 | 1604 | 1699.7 | -12 |
| 01A-64 | 852102 | 397639 | 1898.1 | 1517.7 | 1684.1 | -20 |
| 01A-68 | 279110 | 112001 | 1876.5 | 1795.1 | 1832.9 | -4 |
| 01A-69 | 598461 | 121445 | 1812.5 | 1640.6 | 1717.2 | -9 |
| 01A-70 | 1669071 | 300913 | 1807.5 | 1537.8 | 1654.9 | -15 |
| 01A-71 | 1107438 | 170828 | 1919.6 | 1682.9 | 1790.9 | -12 |
| 01A-72 | 931574 | 57152 | 1786.9 | 1664.5 | 1719.2 | -7 |

| | | | | | | |
|---|---|---|---|---|---|---|
| 01A76 | 99610 | 25666 | 1839.1 | 1921.4 | 1882.3 | 4 |
| 01A79 | 571713 | 555265 | 1942.7 | 1088.5 | 1412.8 | -44 |
| 01A84 | 1100846 | 245820 | 1801 | 1674.9 | 1731.6 | -7 |
| 01A86 | 402521 | 91878 | 1803.3 | 1639.9 | 1712.8 | -9 |
| 01A88 | 710554 | 138228 | 1818.1 | 1769.1 | 1791.7 | -3 |
| 01A90 | 939335 | 26608 | 1927.4 | 1887.1 | 1906.4 | -2 |
| 01A91 | 631499 | 58647 | 1822.4 | 1589.8 | 1692.6 | -13 |
| 01A93 | 677628 | 130204 | 1837.4 | 1702.2 | 1763.7 | -7 |
| 01A94 | 36495 | 15218 | 1854.4 | 1768.5 | 1808.2 | -5 |
| 01A96 | 2553193 | 182227 | 2168.2 | 362.7 | 743.2 | -83 |
| 01A100 | 416609 | 10831 | 1802.6 | 1582 | 1679 | -12 |
| 01A102 | 401821 | 90404 | 1830 | 1703.1 | 1760.7 | -7 |
| 01A107 | 58517 | 68821 | 1848.2 | 1856.4 | 1852.5 | 0 |
| 01A108 | 172429 | 38447 | 1870.2 | 1716.8 | 1787.2 | -8 |
| 01A109 | 774781 | 156559 | 1836 | 1686.7 | 1754.3 | -8 |
| 01A110 | 302032 | 183420 | 1801.5 | 1669.1 | 1728.8 | -7 |
| 01A111 | 137668 | 52754 | 1844.6 | 1595.3 | 1706 | -14 |
| 01A115 | 1114750 | 53076 | 1818.6 | 1650.4 | 1725.9 | -9 |
| 01A119 | 730343 | 121368 | 1892.6 | 1809.7 | 1848.6 | -4 |
| 01A120 | 718614 | 282428 | 1815.9 | 1447.1 | 1603.7 | -20 |
| 01A124 | 458743 | 72170 | 1843.7 | 1773.9 | 1805.9 | -4 |
| 01A125 | 962487 | 48188 | 1898.7 | 1327.3 | 1563.3 | -30 |
| 01A129 | 43937 | 39464 | 1831.3 | 1730.2 | 1776.4 | -6 |
| 01A132 | 492575 | 158796 | 1839.3 | 1616.3 | 1715.6 | -12 |
| 01A136 | 639746 | 216500 | 1839.5 | 1547.4 | 1675.5 | -16 |
| 01A138 | 957689 | 133432 | 1803.9 | 1682.5 | 1737.5 | -7 |
| 01A140 | 868041 | 116475 | 1913.2 | 1266 | 1528.3 | -34 |
| 01A141 | 680987 | 142511 | 1809.4 | 1691.9 | 1745.1 | -6 |
| 01A142 | 178653 | 21761 | 1800.3 | 1740.8 | 1768.1 | -3 |
| 01A143 | 495595 | 76130 | 1834.8 | 1648.8 | 1732.5 | -10 |
| 01A145 | 703193 | 214417 | 1805.8 | 1717.5 | 1757.6 | -5 |
| 01A146 | 492780 | 74051 | 1879.7 | 1170.1 | 1446.3 | -38 |
| 01A148 | 300444 | 93769 | 1835.9 | 1683.3 | 1752.4 | -8 |
| 01A149 | 261046 | 59852 | 1808.5 | 1777.4 | 1791.7 | -2 |
| 01A150 | 348985 | 58389 | 1801.1 | 1723 | 1758.6 | -4 |
| 01A151 | 917639 | 229411 | 1850.2 | 969.1 | 1279.9 | -48 |
| 01A153 | 387430 | 232141 | 1921.9 | 1407.8 | 1626.6 | -27 |
| 01A157 | 824304 | 193580 | 1803.7 | 1700.8 | 1747.6 | -6 |
| 01A161 | 392204 | 105142 | 1932.8 | 1841.7 | 1884.9 | -5 |
| 01A164 | 45025 | 16897 | 1892.6 | 1737.3 | 1808.9 | -8 |
| 11A07 | 362853 | 172410 | 1803.3 | 1676.4 | 1733.5 | -7 |
| 11A09 | 664093 | 191716 | 1823.8 | 1691.7 | 1751.6 | -7 |
| 11A14 | 197214 | 120999 | 1835.5 | 1751 | 1789.8 | -5 |
| 11A33 | 947836 | 188437 | 1838.1 | 1850 | 1844.3 | 1 |

| | | | | | | |
|---|---|---|---|---|---|---|
| 11A34 | 2266715 | 2812586 | 1828.6 | 1432.4 | 1600 | -22 |
| 11A35 | 908283 | 166056 | 1823.1 | 1849.8 | 1837.2 | 1 |
| 11A39 | 880198 | 204848 | 1801.6 | 1659 | 1722.9 | -8 |
| 11A41 | 1786176 | 562777 | 1790.7 | 1793.2 | 1791.9 | 0 |
| 11A44 | 1708308 | 618404 | 1846.2 | 1701 | 1767 | -8 |
| 11A46 | 1059281 | 469429 | 1828.6 | 1832 | 1830.3 | 0 |
| 11A47 | 720564 | 844006 | 1876.4 | 1749.1 | 1807.8 | -7 |
| 28a07 | 183233 | 105198 | 2333.1 | 2283.5 | 2309.7 | -2 |
| 28-13 | 471923 | 295519 | 1941.5 | 1785.4 | 1858.4 | -8 |
| 28-14 | 251278 | 171519 | 1885 | 1783.8 | 1830.8 | -5 |
| 28A27 | 344456 | 87452 | 1814.6 | 1718.2 | 1762.3 | -5 |
| 28A28 | 245934 | 126599 | 1880.5 | 1740.4 | 1805.1 | -7 |
| 28A30 | 1160272 | 212775 | 1815.6 | 1734.2 | 1771.5 | -4 |
| 28A37 | 354470 | 35251 | 1903.8 | 1783.1 | 1839.5 | -6 |
| 28A39 | 286059 | 47014 | 1883.4 | 1785.8 | 1831.1 | -5 |
| 28A43 | 303917 | 45023 | 2295.7 | 2112.3 | 2206.5 | -8 |
| 28A44 | 1145904 | 188666 | 1796.7 | 1795.9 | 1796.1 | 0 |
| 28A45 | 570608 | 211303 | 1800.8 | 1674.6 | 1731.4 | -7 |
| 28A48 | 339849 | 158856 | 1860.4 | 1788.6 | 1821.9 | -4 |
| 28A50 | 1082068 | 206202 | 1825.9 | 1725.8 | 1771.4 | -5 |
| 28A51 | 897922 | 223864 | 1923.1 | 1872.8 | 1896.6 | -3 |
| 28A54 | 355855 | 232315 | 1822.8 | 1719.7 | 1766.6 | -6 |
| 28A55 | 331283 | 101365 | 2379.9 | 2219.2 | 2303.8 | -7 |
| 28A57 | 1259711 | 733735 | 2432.7 | 2185.6 | 2315.7 | -10 |
| 28A67 | 579475 | 175784 | 1859.4 | 1757 | 1804.2 | -6 |
| 28A69 | 679060 | 219764 | 2066.8 | 2012 | 2039.1 | -3 |
| 28A71 | 313965 | 88885 | 1815.9 | 1739.3 | 1774.2 | -4 |
| 28A86 | 196970 | 101154 | 2647 | 2483.1 | 2574.1 | -6 |
| 28A87 | 179246 | 41376 | 1900.5 | 1734.5 | 1810.9 | -9 |
| 28A88 | 587576 | 136461 | 1986.7 | 1809.9 | 1893.4 | -9 |
| 28A89 | 361295 | 209874 | 1865.3 | 1702.9 | 1776.9 | -9 |
| 28A90 | 69956 | 42224 | 2456.1 | 2279.2 | 2373.6 | -7 |
| 28A93 | 647487 | 284850 | 1817 | 1666.7 | 1734.1 | -8 |
| 28A99 | 1162907 | 174194 | 1837.1 | 1932.4 | 1886.8 | 5 |
| 28A101 | 872570 | 710453 | 2055.8 | 1922.8 | 1987.7 | -6 |
| 28A103 | 790657 | 260244 | 1800.2 | 1765 | 1781.1 | -2 |
| 28A105 | 818593 | 222082 | 1814.4 | 1886.8 | 1852.5 | 4 |
| 28A109 | 1125711 | 1197720 | 1817.8 | 1631 | 1714.3 | -10 |
| 28A117 | 275423 | 98613 | 1871.8 | 1901.2 | 1887.1 | 2 |
| 28A118 | 150183 | 56097 | 2281.6 | 2318.8 | 2299 | 2 |
| 28A121 | 596550 | 184413 | 1936.9 | 1863.6 | 1898.4 | -4 |
| 28A134 | 249746 | 229881 | 2305.1 | 2178.6 | 2244.3 | -5 |
| 28A139 | 399104 | 151632 | 1860 | 1833.1 | 1845.7 | -1 |

**Aloolya Gneiss**

| | | | | | | |
|---|---|---|---|---|---|---|
| Igneous Crystallisation | | | | | | |
| 19A01 | 3646528 | 3041320 | 1783.2 | 1628.8 | 1697.2 | -9 |
| 19A06 | 6461809 | 1135694 | 1775.3 | 1771.2 | 1773 | 0 |
| 19A08 | 688602 | 143446 | 1779 | 1647.7 | 1706.2 | -7 |
| 19A09 | 2706423 | 491974 | 1790 | 1655 | 1715.3 | -8 |
| 19A10 | 3896179 | 531945 | 1761.1 | 1757 | 1758.8 | 0 |
| 19-19 | 2142948 | 151677 | 1767.1 | 1774.4 | 1771 | 0 |
| 19A25 | 1747680 | 211905 | 1767 | 1596 | 1671.2 | -10 |
| 19A30 | 2000106 | 254706 | 1785.9 | 1704.6 | 1741.2 | -5 |
| 19A41 | 2114325 | 330479 | 1764.9 | 1752 | 1757.7 | -1 |
| 19A43 | 735912 | 356137 | 1793 | 1675.5 | 1728.2 | -7 |
| 19A66 | 607137 | 179733 | 1757.8 | 1639 | 1691.7 | -7 |
| 19A71 | 1163523 | 302820 | 1797.3 | 1694.1 | 1740.7 | -6 |
| 19A72 | 3169928 | 1632885 | 1796.8 | 1646.3 | 1713.5 | -8 |
| 19A75 | 1267005 | 226001 | 1780.1 | 1685.5 | 1728 | -5 |
| 19A100 | 1225719 | 1110492 | 1766.7 | 1630.9 | 1691 | -8 |
| 19A105 | 2481867 | 459396 | 1795.2 | 1723.6 | 1756.1 | -4 |
| Inherited Zircons | | | | | | |
| 19-18 | 508546 | 150358 | 1831 | 1791.8 | 1809.9 | -2 |
| 19-20 | 1472679 | 978208 | 1987.4 | 1801 | 1889.1 | -9 |
| 19A22 | 296357 | 116143 | 1823.2 | 1889.8 | 1858.1 | 4 |
| 19A28 | 502183 | 453500 | 2183.1 | 2164.2 | 2173.8 | -1 |
| 19A29 | 451070 | 380932 | 2193.3 | 2023.3 | 2108.6 | -8 |
| 19A34 | 748247 | 282988 | 1810.4 | 1696.8 | 1748.2 | -6 |
| 19A36 | 576284 | 138221 | 1857.5 | 1719.6 | 1782.6 | -7 |
| 19A58 | 906278 | 206258 | 2207.3 | 2174.1 | 2191.2 | -2 |
| 19A62 | 994218 | 597922 | 2029.6 | 1855.2 | 1938.9 | -9 |
| 19A83 | 510069 | 47444 | 2261.2 | 2120.2 | 2192.4 | -6 |
| 19A84 | 460895 | 81528 | 1898.1 | 1772 | 1830.4 | -7 |
| 19A90 | 2231188 | 1591779 | 1837.8 | 1671.4 | 1746.4 | -9 |
| 19A98 | 1621350 | 258204 | 1908.4 | 1895.9 | 1901.7 | -1 |
| 19A101 | 2435859 | 409254 | 1894.2 | 1826.1 | 1858 | -4 |
| 19A102 | 1099263 | 843107 | 1810.2 | 1777.8 | 1792.6 | -2 |
| **Un-named Granite** | | | | | | |
| Igneous Crystallisation | | | | | | |
| 36A02 | 406632 | 31024 | 1768.6 | 1737.4 | 1751.8 | -2 |
| 36A03 | 286400 | 33334 | 1798.2 | 1797.8 | 1798.1 | 0 |
| 36A04 | 219691 | 71840 | 1771.1 | 1720.4 | 1743.6 | -3 |
| 36A05 | 309322 | 110409 | 1800.3 | 1640.7 | 1712.1 | -9 |
| 36A07 | 346997 | 42622 | 1791 | 1788.3 | 1789.6 | 0 |
| 36A08 | 276451 | 35558 | 1762.3 | 1770.6 | 1766.8 | 0 |
| 36A10 | 287600 | 18746 | 1780.9 | 1751.7 | 1765.1 | -2 |
| 36A15 | 732389 | 99886 | 1757.4 | 1738.7 | 1746.9 | -1 |
| 36A16 | 685146 | 94854 | 1783.8 | 1690.8 | 1732.5 | -5 |

| | | | | | | |
|---|---|---|---|---|---|---|
| 36A20 | 496617 | 59109 | 1768.1 | 1832.8 | 1802.4 | 4 |
| 36A21 | 113135 | 61624 | 1752.6 | 1802.5 | 1779.1 | 3 |
| 36A26 | 283659 | 37776 | 1771.8 | 1754.2 | 1762.1 | -1 |
| 36A27 | 212395 | 21459 | 1763 | 1752 | 1756.8 | -1 |
| 36A30 | 240967 | 37144 | 1754.1 | 1701.4 | 1725 | -3 |
| 36A32 | 534685 | 40707 | 1774.6 | 1706.9 | 1737.3 | -4 |
| 36A33 | 434593 | 83948 | 1778.8 | 1748.2 | 1762 | -2 |
| 36A34 | 212993 | 32324 | 1783.5 | 1674.9 | 1723.5 | -6 |
| 36A36 | 376701 | 370175 | 1788.4 | 1767.1 | 1776.7 | -1 |
| 36A38 | 381989 | 61392 | 1803.4 | 1766.1 | 1783 | -2 |
| 36A41 | 217908 | 17360 | 1790.6 | 1761 | 1774.5 | -2 |
| 36A42 | 310067 | 173114 | 1794.6 | 1736.4 | 1762.9 | -3 |
| 36A43 | 400101 | 63477 | 1794.8 | 1774.3 | 1783.7 | -1 |
| 36A46 | 369396 | 42459 | 1789.9 | 1778.4 | 1783.6 | -1 |
| 36A47 | 357172 | 51896 | 1754.7 | 1729.6 | 1740.9 | -1 |
| 36A50 | 317595 | 70032 | 1783.1 | 1751 | 1765.6 | -2 |
| 36A51 | 635196 | 62184 | 1760.3 | 1693.9 | 1723.7 | -4 |
| 36A52 | 499305 | 25405 | 1786.9 | 1746.2 | 1764.7 | -2 |
| 36A54 | 349802 | 52301 | 1781.5 | 1753.1 | 1766 | -2 |
| 36A58 | 203756 | 26187 | 1773.9 | 1737.6 | 1754.2 | -2 |
| 36A62 | 253784 | 47264 | 1789.2 | 1743.2 | 1764.2 | -3 |
| 36A63 | 438560 | 47867 | 1751.2 | 1749 | 1749.9 | 0 |
| 36A64 | 400426 | 40812 | 1795.2 | 1754.3 | 1772.9 | -2 |
| 36A66 | 146005 | 25611 | 1760.5 | 1699.8 | 1727 | -3 |
| 36A67 | 323500 | 39788 | 1761.8 | 1770.4 | 1766.2 | 0 |
| 36A68 | 268317 | 21501 | 1764.5 | 1717.5 | 1738.6 | -3 |
| 36A69 | 338973 | 43201 | 1783.8 | 1742.5 | 1761.1 | -2 |
| 36A70 | 211261 | 173941 | 1789.7 | 1721.2 | 1752.1 | -4 |
| 36A71 | 297114 | 84948 | 1776.3 | 1733.4 | 1752.8 | -2 |
| 36A73 | 161061 | 21949 | 1771.9 | 1749.2 | 1759.4 | -1 |
| 36A75 | 381279 | 24154 | 1805 | 1785.3 | 1794.2 | -1 |
| 36A77 | 275005 | 33248 | 1799.4 | 1737.9 | 1765.8 | -3 |
| 36A79 | 323530 | 90884 | 1754.4 | 1757.3 | 1755.6 | 0 |
| 36A84 | 306774 | 54483 | 1767.1 | 1741.2 | 1753 | -1 |
| 36A86 | 429079 | 48465 | 1770.9 | 1762.2 | 1766.2 | 0 |
| 36A90 | 811228 | 125274 | 1785.8 | 1764.2 | 1774.1 | -1 |
| 36A100 | 177582 | 110497 | 1794.6 | 1780.9 | 1786.9 | -1 |
| 36A101 | 1193731 | 122958 | 1799.4 | 1731 | 1761.9 | -4 |
| 36A103 | 671046 | 52895 | 1770.1 | 1768.1 | 1768.8 | 0 |
| 36A104 | 392081 | 44193 | 1781.2 | 1818.1 | 1800.7 | 2 |
| 36A105 | 368779 | 38401 | 1754.7 | 1759 | 1756.8 | 0 |
| 36A108 | 345895 | 50766 | 1802.9 | 1852.5 | 1829.1 | 3 |
| 36A110 | 419313 | 189040 | 1804.3 | 1875.1 | 1841.6 | 4 |
| 36A111 | 677712 | 63624 | 1805.3 | 1856.2 | 1832.2 | 3 |

| | | | | | | |
|---|---|---|---|---|---|---|
| 36A116 | 318746 | 60827 | 1755.6 | 1801.8 | 1780.4 | 3 |
| 36A118 | 204731 | 49159 | 1764.7 | 1830.8 | 1800.1 | 4 |
| 36A120 | 199703 | 121587 | 1750.3 | 1771.5 | 1761.7 | 1 |
| 36A121 | 409087 | 74110 | 1760.9 | 1784.3 | 1773.5 | 1 |
| 36A125 | 978490 | 79354 | 1784.7 | 1874 | 1832 | 5 |
| 36A126 | 857758 | 48014 | 1805.8 | 1840.9 | 1824.5 | 2 |
| 36A127 | 515183 | 87627 | 1797 | 1819.5 | 1809.1 | 1 |
| Inherited Zircons | | | | | | |
| 36A06 | 914931 | 70217 | 1828.6 | 1852.7 | 1841.6 | 1 |
| 36A09 | 1299382 | 419848 | 1888.2 | 1919.4 | 1904.5 | 2 |
| 36A13 | 176737 | 76390 | 1840.5 | 1869.5 | 1855.6 | 2 |
| 36A17 | 682819 | 108737 | 2087.3 | 2019.4 | 2052.9 | -3 |
| 36A25 | 313072 | 190818 | 1989.4 | 1884.9 | 1934.6 | -5 |
| 36A29 | 198429 | 68993 | 1835.1 | 1837.5 | 1836.2 | 0 |
| 36A31 | 159585 | 25840 | 1825.9 | 1748.6 | 1783.9 | -4 |
| 36A37 | 182010 | 31543 | 1853.2 | 1805.3 | 1827.5 | -3 |
| 36A38 | 381989 | 61392 | 1803.4 | 1766.1 | 1783 | -2 |
| 36A39 | 259774 | 134120 | 1819 | 1765.2 | 1789.8 | -3 |
| 36A240 | 177931 | 64240 | 1875.7 | 1820.1 | 1846 | -3 |
| 36A48 | 262345 | 45688 | 2342.8 | 2188.4 | 2269.1 | -7 |
| 36A49 | 333487 | 83429 | 1693.6 | 1678.6 | 1685.2 | -1 |
| 36A53 | 82986 | 25327 | 3114 | 2985 | 3062.5 | -4 |
| 36A60 | 599041 | 32926 | 1842.5 | 1741.4 | 1787.8 | -5 |
| 36A72 | 305974 | 22112 | 1840.4 | 1781.4 | 1808.6 | -3 |
| 36A74 | 216219 | 20557 | 1918.2 | 1838.5 | 1875.9 | -4 |
| 36A75 | 381279 | 24154 | 1805 | 1785.3 | 1794.2 | -1 |
| 36A80 | 237756 | 69800 | 1821.9 | 1737.3 | 1776.1 | -5 |
| 36A82 | 211918 | 147361 | 1812.8 | 1783.5 | 1797 | -2 |
| 36A87 | 301892 | 146679 | 1937.9 | 1874.2 | 1904.6 | -3 |
| 36A89 | 353928 | 53991 | 1860.4 | 1867.3 | 1864 | 0 |
| 36A91 | 138533 | 79782 | 1857 | 1819.2 | 1836.8 | -2 |
| 36A92 | 148508 | 130958 | 2416.6 | 2419.8 | 2417.6 | 0 |
| 36A93 | 726946 | 512042 | 1838.7 | 1891.7 | 1866.1 | 3 |
| 36A94 | 1431898 | 83006 | 2791.2 | 2738.1 | 2768.3 | -2 |
| 36A95 | 139608 | 67235 | 1831.8 | 1827.8 | 1829.2 | 0 |
| 36A97 | 210817 | 89875 | 1901.3 | 1905.9 | 1903.3 | 0 |
| 36A99 | 190749 | 96225 | 1809.5 | 1807 | 1807.7 | 0 |
| 36A102 | 502369 | 66323 | 1815.8 | 1793.8 | 1803.7 | -1 |
| 36A106 | 293085 | 132014 | 1822.6 | 1843.1 | 1833.3 | 1 |
| 36A107 | 865015 | 234499 | 1854.8 | 1893.7 | 1875 | 2 |
| 36A108 | 345895 | 50766 | 1802.9 | 1852.5 | 1829.1 | 3 |
| 36A109 | 314965 | 166169 | 1846.4 | 1858.1 | 1852.4 | 1 |
| 36A110 | 419313 | 189040 | 1804.3 | 1875.1 | 1841.6 | 4 |
| 36A111 | 677712 | 63624 | 1805.3 | 1856.2 | 1832.2 | 3 |

| | | | | | | |
|---|---|---|---|---|---|---|
| 36A112 | 284223 | 38417 | 2028.5 | 1998.8 | 2013.3 | -1 |
| 36A113 | 237349 | 104292 | 1819.4 | 1790.3 | 1803.7 | -2 |
| 36A114 | 73098 | 21647 | 2604.4 | 2615.7 | 2609.2 | 0 |
| 36A117 | 117993 | 39128 | 2495.7 | 2364.8 | 2435.7 | -5 |
| 36A124 | 416427 | 183615 | 1956.6 | 1953.7 | 1955 | 0 |
| 36A126 | 857758 | 48014 | 1805.8 | 1840.9 | 1824.5 | 2 |
| 36A128 | 1448232 | 511134 | 2000.7 | 2034.7 | 2017.9 | 2 |